NASA MEMO 12-4-58A

NASA

MEMORANDUM

THREE-DIMENSIONAL ORBITS OF EARTH SATELLITES, INCLUDING EFFECTS OF EARTH OBLATENESS AND ATMOSPHERIC ROTATION

By Jack N. Nielsen, Frederick K. Goodwin, and William A. Mersman

Ames Research Center
Moffett Field, Calif.

NATIONAL AERONAUTICS AND SPACE ADMINISTRATION
WASHINGTON
December 1958

L

12-4-58A

TABLE OF CONTENTS

NATIONAL AERONAUTICS AND SPACE ADMINISTRATION

MEMORANDUM 12-4-58A

THREE-DIMENSIONAL ORBITS OF EARTH SATELLITES, INCLUDING EFFECTS OF EARTH OBLATENESS AND ATMOSPHERIC ROTATION

By Jack N. Nielsen, Frederick K. Goodwin,
and William A. Mersman

SUMMARY

The principal purpose of the present paper is to present sets of equations which may be used for calculating complete trajectories of earth satellites from outer space to the ground under the influence of air drag and gravity, including oblateness effects, and to apply these to several examples of entry trajectories starting from a circular orbit.

Equations of motion, based on an "instantaneous ellipse" technique, with polar angle as independent variable, were found suitable for automatic computation of orbits in which the trajectory consists of a number of revolutions. This method is suitable as long as the trajectory does not become nearly vertical. In the terminal phase of the trajectories, which are nearly vertical, equations of motion in spherical polar coordinates with time as the independent variable were found to be more suitable.

In the first illustrative example the effects of the oblateness component of the earth's gravitational field and of atmospheric rotation were studied for equatorial orbits. The satellites were launched into circular orbits at a height of 120 miles, an altitude sufficiently high that a number of revolutions could be studied. The importance of the oblateness component of the earth's gravitational field is shown by the fact that a satellite launched at circular orbital speed, neglecting oblateness, has a perigee some 67,000 feet lower when oblateness forces are included in the equations of motion than when they are not included. Also, the loss in altitude per revolution is double that of a satellite following an orbit not subject to oblateness. The effect of atmospheric rotation on the loss of altitude per revolution was small. As might be surmised, the regression of the line of nodes as predicted by celestial mechanics is unchanged when drag is included. It is clear that the inclination of the orbital plane to the equator will be relatively unaffected by drag for no atmospheric rotation since the drag lies in the orbital plane in this case. With the inclusion of atmospheric rotation it was found that the inclination of the plane changed about one-millionth of a radian per revolution. Thus the prediction of the

position of the orbital plane of an earth satellite is not complicated by the introduction of drag. The line of apsides, which without drag but with oblateness moves slowly in space, tends to move with the satellite when drag is included in the calculations. As a results, the usual linearized solutions based on oblateness alone must be basically altered when drag is included to take into account the rapid movement of the line of apsides.

In the second illustrative example the final revolution was calculated to impact for a number of trajectories in an orbital plane inclined at 65° to the equator. Of particular interest is the large effect the oblateness gravitational field and atmospheric rotation can have on the impact point. For a value of C_DA/m of unity, and for an initial downward angle at 80 miles altitude of 0.01 radian, such as might be utilized for manned re-entry, oblateness had an influence of about 300 miles in the impact point, and atmospheric rotation had about a 150-mile influence.

It was found that two-dimensional solutions neglecting atmospheric rotation can be used to approximate three-dimensional solutions including atmospheric rotation. In this connection two-dimensional theories must be interpreted as being viewed by an observer on a rotating earth.

The importance of various terms in the equations of radial and tangential motion is examined for various calculated trajectories. The validity of the principal assumption in the approximate equation of motion of TN 4276 was thus confirmed for a satellite speed less than about 99-percent circular satellite velocity. Certain gaps in our theoretical and experimental knowledge are pointed out insofar as they influence our ability to calculate complete trajectories from launch to impact.

INTRODUCTION

Much interest exists in the dynamics of earth satellites, and a number of papers (e.g., refs. 1 to 6) in the field have recently appeared. These papers consider only parts of the total trajectory; they are also usually limited to two-dimensional trajectories, or they neglect air drag. The principal purpose of this paper is to present sets of equations which may be used for the calculations of complete trajectories from outer space to the ground under the influences of air drag and gravity, including oblateness effects, and to apply these to several illustrative examples of entry trajectories starting from a circular orbit. This purpose cannot be achieved at present on the basis of analytical solutions except possibly by patching together such solutions. Therefore, automatic computing machinery was used in the study. Forms of the equations of motion suitable for automatic computation are presented, and a number of calculative examples are carried out. The calculative examples are chosen to illustrate the relative importance of various physical forces acting on earth

satellites. Some of the essential physical features of the calculated solutions are discussed in the hope that the resulting insight will lead to more inclusive analytical solutions. In connection with the numerical calculations the authors wish to acknowledge the contributions of Miss Marcelline Chartz in programing the equations for the digital computing machines and in supervising the computations.

SYMBOLS

a	equatorial radius of earth
a_r, a_λ, a_ψ	components of acceleration vector along $\vec{i}_r, \vec{i}_\lambda$, and $\vec{i}_\psi$ directions
A	reference area of satellite
$\vec{A}$	acceleration vector of satellite
b	polar radius of earth
C_D	drag coefficient
D	drag force
$D_r, D_\lambda, D_\psi, D_\varphi, D_\alpha$	components of drag along $\vec{i}_r, \vec{i}_\lambda, \vec{i}_\psi, \vec{i}_\varphi$, and $\vec{i}_\alpha$ directions
e	eccentricity of earth
E	eccentricity of instantaneous ellipse, $\left(\frac{l^2 - k^2}{l^2}\right)^{1/2}$
E	total energy of satellite
$\vec{F}$	vector force acting on satellite
$F_r, F_\lambda, F_\psi, F_\varphi, F_\alpha$	components of $\vec{F}$ along $\vec{i}_r, \vec{i}_\lambda, \vec{i}_\psi, \vec{i}_\varphi$, and $\vec{i}_\alpha$ directions
g	component of gravity acceleration at earth's surface; no oblateness
$\vec{G}$	vector force per unit mass acting on satellite because of gravity of earth
$G_r, G_\lambda, G_\psi, G_\varphi, G_\alpha$	components of $\vec{G}$ along $\vec{i}_r, \vec{i}_\lambda, \vec{i}_\psi, \vec{i}_\varphi$, and $\vec{i}_\alpha$ directions

Oblateness	3	Yes	Yes	No	Outside atmosphere within range of oblateness forces	2
Circulari-					During circu-	

$\vec{\Omega}$	vector angular velocity of $\vec{i}_r, \vec{i}_\lambda, \vec{i}_\psi$ system in inertial framework
Ω_e	angular velocity of earth about polar axis
$\Delta\vec{\Omega}$	change in angular velocity due to motion of orbital plane
$\Delta\vec{\Omega}_f$	angular velocity for fixed orbital plane

The angle β is the bearing angle of the orbital plane in the r, λ, ψ system. The bearing angle for an earth observer is different from β because of earth rotation.

The relationships among the various angles can be readily established. The following six relationships are useful

$$\sin \psi = \sin \varphi \sin \alpha$$

$$\sin(\lambda - \theta) = \frac{\sin \varphi \cos \alpha}{\cos \psi}$$

$$\cos(\lambda - \theta) = \frac{\cos \varphi}{\cos \psi}$$

$$\sin \alpha \cos \varphi = \cos \psi \cos \beta$$

$$\cos \alpha = \cos \psi \sin \beta$$

$$\tan \alpha = \frac{\tan \psi}{\sin(\lambda - \theta)}$$

The direction cosines between the r, φ, α system and the r, λ, ψ system are

	r	φ	α
r	1	0	0
λ	0	$\sin \beta$	$-\cos \beta$
ψ	0	$\cos \beta$	$\sin \beta$

Properties of the Atmosphere and the Earth

The forces due to air drag depend on the density and rotation of the atmosphere, and the forces due to gravitation depend on the size, shape, and density distribution of the earth. The atmospheric properties that are adopted for the exact calculations of this report are those contained in reference 9. However, as a result of observation of the satellite 1957 α_2, Sputnik I, the ARDC densities above about 200 KM appear to

will be a periodic variation in density for a purely circular orbit, due to the nonspherical figure of the earth, except for equatorial orbits. For a polar orbit, for instance, there would be density changes between the equator and the poles corresponding to a 13-mile change in altitude for a circular orbit. We consider this density change to be due to the nonspherical figure of the earth and do not call it an oblateness effect, a term applying only to the gravitational field.

In the calculations it is necessary to know the size and shape of the earth. It is assumed that the earth is an ellipsoid (oblate spheroid) with the dimensions adopted at the International Geodetic and Geophysical Union of 1924, as given in reference 8. The equator is assumed to be a perfect circle of radius a, and the polar radius is b.

$$\left.\begin{aligned} a &= 6{,}378{,}388 \pm 18 \text{ meters} \\ &= 3963.3386 \text{ statute miles} \\ &= 20{,}926{,}428 \text{ feet} \\ b &= 6{,}356{,}911.946 \text{ meters} \\ &= 3949.9941 \text{ statute miles} \\ &= 20{,}855{,}969 \text{ feet} \end{aligned}\right\} \tag{4}$$

$$\frac{a-b}{a} = \frac{1}{297} = 0.003367003^4 \tag{5}$$

$$e^2 = \frac{a^2 - b^2}{a^2} = 0.0067226700 \tag{6}$$

(1 meter = 3.28083333 feet)

It is also necessary to specify a value of the earth's gravitational field strength for the purposes of the calculations. If F is the gravitation attraction between two masses M and m a distance r apart, then the universal gravitational constant K is given by

$$F = K \frac{Mm}{r^2}$$

If g is the force on a unit mass due to the earth's gravitational field at the surface of the earth, M the mass of the earth, and r is equal to R, the "mean" radius of the earth, then

$$KM = gR^2$$

It turns out that we shall have use of the quantity KM which is given in reference 11 as

$$\left.\begin{aligned} KM &= (1 \pm 8\times10^{-5})(3.986329\times10^{20}\ cm^3/sec^2) \\ KM &= 0.14077500\times10^{17}\ ft^3/sec^2 \end{aligned}\right\} \qquad (7)$$

Another quantity of the earth's gravitational field with which we will be concerned is its quadripole moment. Because of the nonspherical mass distribution of the earth, its gravitational field is not spherically symmetric, but has a quadripole moment. The potential is that due to a quadripole formed as shown in the sketch. A quartet of sources and sinks with strengths of equal magnitude are placed on the polar axis of the earth near its center. The sources are located at the center with the sinks equally spaced above and below the center. The sinks are permitted to approach the sources while the product of strength and spacing remains constant. The net result is a quadripole of the present sort which resembles a dipole pair with mirror symmetry. Also shown in the sketch are the radial and tangential components of the gravitational field due to oblateness. The gravitational potential including the nonspherical component is usually taken as

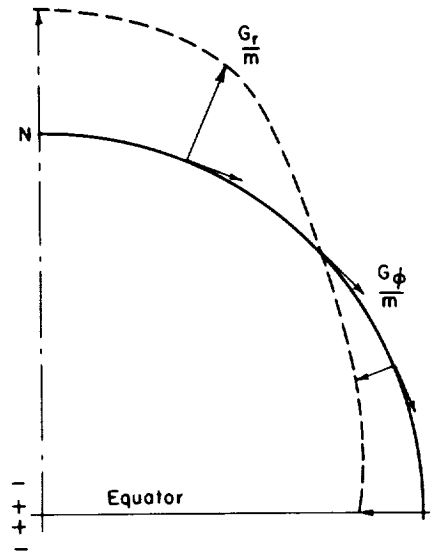

Sketch (a)

$$\Phi = \frac{KM}{r}\left[1 - \frac{\mu a^2}{r^2}(1 - 3\cos 2\psi)\right] \qquad (8)$$

The force per unit mass in any direction is the gradient of Φ. The value ψ is the geocentric latitude and μ is a dimensionless constant given in reference 2 as

$$6\mu = (1.637 \pm 0.004)\times10^{-3}$$

From reference 11, a value of 6μ calculated for the international ellipsoid is

$$6\mu = 1.638\times10^{-3}$$

We will use this value in the calculations.

It is probably interesting to note that the surfaces for which Φ is a constant are not oblate spheroids nor does one coincide with the assumed geometric figure of the earth. The surfaces, Φ equal to a constant, in principle are everywhere normal to the earth's gravitational field. If the vector gravitational field is corrected for the acceleration due to rotation of the earth, then the resultant vector field should be normal to the "mean" surface of the oceans to prevent their flowing toward the equator.

If we designate the gravitational force per unit mass in the $\vec{i}_r$, $\vec{i}_\lambda$, $\vec{i}_\psi$, $\vec{i}_\varphi$, and $\vec{i}_\alpha$ directions by G_r/m, G_λ/m, G_ψ/m, G_φ/m, and G_α/m, we have in the r, λ, ψ system

$$\left.\begin{aligned} \frac{G_r}{m} &= \frac{\partial \Phi}{\partial r} = -\frac{KM}{r^2} + \frac{3\mu KMa^2}{r^4}(1 - 3\cos 2\psi) \\ \frac{G_\lambda}{m} &= \frac{1}{r\cos\psi}\frac{\partial \Phi}{\partial \lambda} = 0 \\ \frac{G_\psi}{m} &= \frac{1}{r}\frac{\partial \Phi}{\partial \psi} = -\frac{6KM\mu a^2}{r^4}\sin 2\psi \end{aligned}\right\} \tag{9}$$

In the r, φ, α system we have

$$\left.\begin{aligned} \frac{G_r}{m} &= -\frac{KM}{r^2} - \frac{6\mu KMa^2}{r^4}(1 - 3\sin^2\varphi \sin^2\alpha) \\ \frac{G_\varphi}{m} &= -\frac{12KM\mu a^2}{r^4}\sin\varphi\cos\varphi\sin^2\alpha \\ \frac{G_\alpha}{m} &= -\frac{12KM\mu a^2}{r^4}\sin\varphi\cos\alpha\sin\alpha \end{aligned}\right\} \tag{10}$$

The equations are obtained by noting that G_φ and G_α can easily be obtained from G_λ and G_ψ by a rotation involving β (see fig. 1(a)). The quantities ψ and β are then eliminated in favor of φ and α through relationships derivable on the basis of spherical trigonometry.

Air Drag Forces

Besides the forces on the satellite due to the gravitational field of the earth, we will also be concerned with the air drag on the satellite with the atmosphere rotating with the earth. In the r, λ, ψ system the velocity of the satellite relative to the rotating atmosphere, $\vec{V}_R$, is

$$\vec{V}_R = \vec{i}_r\dot{r} + \vec{i}_\lambda r\cos\psi(\dot{\lambda} - \Omega_e) + \vec{i}_\psi r\dot{\psi} \tag{11}$$

where Ω_e is the rotational speed of the earth. Since the drag is in opposition to the motion

$$\frac{D}{m} = -\frac{1}{2}\rho V_R^2\left(\frac{C_D A}{m}\right) \tag{12}$$

The components of the drag in the r, λ, ψ system are thus

$$\left.\begin{aligned} \frac{D_r}{m} &= -\frac{1}{2}\rho V_R \dot{r}\left(\frac{C_D A}{m}\right) \\ \frac{D_\lambda}{m} &= -\frac{1}{2}\rho V_R r\cos\psi(\dot{\lambda}-\Omega_e)\left(\frac{C_D A}{m}\right) \\ \frac{D_\psi}{m} &= -\frac{1}{2}\rho V_R r\dot{\psi}\left(\frac{C_D A}{m}\right) \end{aligned}\right\} \tag{13}$$

In the r, φ, α system the velocity $\vec{V}_R$ is (as we will show)

$$\begin{aligned} \vec{V}_R &= \vec{i}_r\dot{r} + \vec{i}_\varphi V_\varphi - \vec{i}_\lambda r\Omega_e\cos\psi \\ &= \vec{i}_r\dot{r} + \vec{i}_\varphi V_\varphi - r\Omega_e\cos\psi(\vec{i}_\varphi\sin\beta - \vec{i}_\alpha\cos\beta) \\ &= \vec{i}_r\dot{r} + \vec{i}_\varphi(V_\varphi - r\Omega_e\cos\alpha) + \vec{i}_\alpha r\Omega_e\sin\alpha\cos\varphi \end{aligned} \tag{14}$$

where we have made use of the relationships

$$\left.\begin{aligned} \sin\beta\cos\psi &= \cos\alpha \\ \cos\beta\cos\psi &= \sin\alpha\cos\varphi \end{aligned}\right\} \tag{15}$$

The drag components per unit mass in the r, φ, α system are thus

$$\left.\begin{aligned} \frac{D_r}{m} &= -\frac{1}{2}\rho V_R \dot{r}\left(\frac{C_D A}{m}\right) \\ \frac{D_\varphi}{m} &= -\frac{1}{2}\rho V_R(V_\varphi - r\Omega_e\cos\alpha)\left(\frac{C_D A}{m}\right) \\ \frac{D_\alpha}{m} &= -\frac{1}{2}\rho V_R r\Omega_e\sin\alpha\cos\varphi\left(\frac{C_D A}{m}\right) \end{aligned}\right\} \tag{16}$$

SATELLITE KINEMATICS AND EQUATIONS OF MOTION

Equations of Motion in Geographical Coordinates

The geographical coordinates r, λ, ψ are a special set of spherical polar coordinates useful for certain problems of trajectory calculations. They are related to the inertial coordinates X, Y, Z as follows:

$$X = r \cos \psi \cos \lambda$$

$$Y = r \cos \psi \sin \lambda$$

$$Z = r \sin \psi$$

The linear velocities in the r, λ, ψ directions (fig. 1(a)) are

$$V_r = \dot{r}$$

$$V_\lambda = r\dot{\lambda} \cos \psi$$

$$V_\psi = r\dot{\psi}$$

and the corresponding components of the angular velocity of the $\vec{i}_r$, $\vec{i}_\lambda$, $\vec{i}_\psi$ coordinate system are

$$\left.\begin{aligned} \Omega_r &= \dot{\lambda} \sin \psi \\ \Omega_\lambda &= -\dot{\psi} \\ \Omega_\psi &= \dot{\lambda} \cos \psi \end{aligned}\right\} \tag{17}$$

The angular velocities referred to here concern rotations of the $\vec{i}_r$, $\vec{i}_\lambda$, $\vec{i}_\psi$ system in the inertial framework. The acceleration components are

$$\left.\begin{aligned} a_r &= \ddot{r} - r\dot{\psi}^2 - r\dot{\lambda}^2 \cos^2 \psi \\ a_\lambda &= \frac{1}{r \cos \psi} \frac{d}{dt} (r^2 \cos^2 \psi \dot{\lambda}) \\ a_\psi &= r\ddot{\psi} + 2\dot{r}\dot{\psi} + r\dot{\lambda}^2 \sin \psi \cos \psi \end{aligned}\right\} \tag{18}$$

The forces per unit mass in r, λ, and ψ directions are equal to the accelerations in those directions, so that the equations of motion are:

$$\left.\begin{aligned} \frac{F_r}{m} &= \ddot{r} - r\dot{\psi}^2 - r\dot{\lambda}^2 \cos^2 \psi \\ \frac{F_\lambda}{m} &= \frac{1}{r \cos \psi} \frac{d}{dt} (r^2 \cos^2 \psi \dot{\lambda}) \\ \frac{F_\psi}{m} &= r\ddot{\psi} + 2\dot{r}\dot{\psi} + r\dot{\lambda}^2 \sin \psi \cos \psi \end{aligned}\right\} \tag{19}$$

Under the actions of gravity, including oblateness, and of air drag the forces per unit mass are

$$\left.\begin{aligned}
\frac{F_r}{m} &= -\frac{KM}{r^2} + \frac{3\mu KMa^2}{r^4}(1 - 3\cos 2\psi) - \frac{1}{2}\rho V_R \dot{r}\left(\frac{C_D A}{m}\right) \\
\frac{F_\lambda}{m} &= -\frac{1}{2}\rho V_R r \cos\psi(\dot{\lambda} - \Omega_e)\left(\frac{C_D A}{m}\right) \\
\frac{F_\psi}{m} &= -\frac{6KM\mu a^2}{r^4}\sin 2\psi - \frac{1}{2}\rho V_R r\dot{\psi}\left(\frac{C_D A}{m}\right)
\end{aligned}\right\} \qquad (20)$$

Equations of Motion in Orbital Plane; Motion of Plane

For certain kinds of calculations the equations of motion in terms of r, φ, and α are convenient. The unit vectors $\vec{i}_r$, $\vec{i}_\varphi$, and $\vec{i}_\alpha$ form a right-handed system in that order. Because the r, φ, α coordinate system is not an inertial system, account must be taken of its rotation in establishing the equations of motion. It is clear that r, φ, α, and θ are necessary to describe the position of the satellite, so that θ will also enter the equations of motion. Let us first establish the kinematic relationships of the system. Since there are four coordinates specifying the satellite position, rather than the usual three, we can anticipate an extra kinematic relationship involving r, φ, α, and θ.

A convenient method for deriving certain kinematic relationships is to obtain the quantity $\vec{\Omega}\times\vec{r}$ by two methods and then to equate its components. One convenient way to establish $\vec{\Omega}\times\vec{r}$ is to consider the following vector transformation between any vector, $\vec{r}$, and its time rate of change

$$\frac{d\vec{r}}{dt} = \frac{\partial\vec{r}}{\partial t} + \vec{\Omega}\times\vec{r} \qquad (21)$$

as discussed, for instance in reference 12. In this equation $d\vec{r}/dt$ is the total rate of change of the vector, $\vec{r}$ including both changes in the magnitudes and directions of its components. The quantity $\partial\vec{r}/\partial t$ refers to the rate of change of $\vec{r}$ due solely to the changes in the magnitudes of its components but with no changes in their directions. The angular velocity, $\vec{\Omega}$, is that of the axis system in which the components are expressed. (The ability to hold the direction of the components fixed presupposes the knowledge of an inertial system to which $\vec{\Omega}$ can be referred.)

Let us now take $\vec{r}$ to be the radius vector of the satellite so that $d\vec{r}/dt$ is the satellite velocity $\vec{V}$. From the definition of the orbital plane, we have in the r, φ, α system

$$\vec{V} = \frac{d\vec{r}}{dt} = \vec{i}_r\dot{r} + \vec{i}_\varphi V_\varphi \qquad (22)$$

The quantity $\partial\vec{r}/\partial t$ is the satellite velocity if the $\vec{i}_r$, $\vec{i}_\varphi$, and $\vec{i}_\alpha$ directions are fixed.

$$\frac{\partial \vec{r}}{\partial t} = \vec{i}_r \dot{r} \tag{23}$$

From equations (21), (22), and (23), we thus obtain

$$\vec{\Omega} \times \vec{r} = \vec{i}_\varphi V_\varphi \tag{24}$$

The second method used to obtain $\vec{\Omega}\times\vec{r}$ is to construct $\vec{\Omega}$ and then to take its cross product with $\vec{r}$. To establish the angular velocity we note that of the independent variables, r, φ, α, θ, changes in all quantities except r cause angular velocity of the moving axes. If we hold the orbital plane fixed in space, we get an angular velocity vector along $\vec{i}_\alpha$ due to $\dot{\varphi}$.

$$\Delta\vec{\Omega}_f = \vec{i}_\alpha \dot{\varphi} = \vec{i}_\alpha \left(\frac{V_\varphi}{r}\right)_f \tag{25}$$

Now, because of motion of the orbital plane specified by $\dot{\theta}$ and $\dot{\alpha}$, we have the additional angular velocity $\Delta\vec{\Omega}$ which is clearly

$$\Delta\vec{\Omega} = \vec{i}_Z \dot{\theta} + \vec{i}_{X'} \dot{\alpha} \tag{26}$$

The vector $\Delta\vec{\Omega}$ can easily be transferred to the r, φ, α system by means of the following table of direction cosines

	r	φ	α
X'	cos φ	-sin φ	0
Y'	sin φ cos α	cos φ cos α	-sin α
Z	sin φ sin α	cos φ sin α	cos α

$$\Delta\vec{\Omega} = \vec{i}_r(\dot{\theta} \sin\varphi \sin\alpha + \dot{\alpha}\cos\varphi) + \vec{i}_\varphi(\dot{\theta}\cos\varphi\sin\alpha - \dot{\alpha}\sin\varphi) + \vec{i}_\alpha(\dot{\theta}\cos\alpha) \tag{27}$$

The total angular velocity is now

$$\vec{\Omega} = \Delta\vec{\Omega}_f + \Delta\vec{\Omega} = \vec{i}_r(\dot{\theta}\sin\varphi\sin\alpha + \dot{\alpha}\cos\varphi) + \vec{i}_\varphi(\dot{\theta}\cos\varphi\sin\alpha - \dot{\alpha}\sin\varphi) + \vec{i}_\alpha(\dot{\varphi} + \dot{\theta}\cos\alpha) \tag{28}$$

If we take the vector product $\vec{\Omega}\times\vec{r}$ from equation (28), we get

$$\vec{\Omega}\times\vec{r} = -\vec{i}_\alpha r(\dot{\theta}\cos\varphi\sin\alpha - \dot{\alpha}\sin\varphi) + \vec{i}_\varphi r(\dot{\varphi} + \dot{\theta}\cos\alpha) \tag{29}$$

Comparison of equations (24) and (29) yields a pair of relationships

$$\left.\begin{aligned} \dot{\theta} \cos \varphi \sin \alpha - \dot{\alpha} \sin \varphi &= 0 \\ \dot{\varphi} + \dot{\theta} \cos \alpha &= \frac{V_\varphi}{r} \end{aligned}\right\} \tag{30}$$

The angular velocity of the satellite is thus

$$\vec{\Omega} = \vec{i}_r \dot{\theta} \frac{\sin \alpha}{\sin \varphi} + \vec{i}_\alpha \left(\frac{V_\varphi}{r}\right)$$

$$= \vec{i}_r \frac{\dot{\alpha}}{\cos \varphi} + \vec{i}_\alpha \left(\frac{V_\varphi}{r}\right) \tag{31}$$

The acceleration in r, φ, α coordinates is derived from a vector transformation equation similar to equation (21)

$$\frac{d\vec{V}}{dt} = \frac{\partial \vec{V}}{\partial t} + \vec{\Omega} \times \vec{V}$$

The quantity, $\partial \vec{V}/\partial t$, with $\vec{i}_r$, $\vec{i}_\varphi$, and $\vec{i}_\alpha$ fixed is

$$\frac{\partial \vec{V}}{\partial t} = \vec{i}_r \ddot{r} + \vec{i}_\varphi \dot{V}_\varphi$$

since the rotation of the moving coordinates do not contribute to $\partial \vec{V}/\partial t$. The vector product $\vec{\Omega} \times \vec{V}$ is

$$\vec{\Omega} \times \vec{V} = \begin{vmatrix} \vec{i}_r & \vec{i}_\varphi & \vec{i}_\alpha \\ \Omega_r & 0 & \frac{V_\varphi}{r} \\ \dot{r} & V_\varphi & 0 \end{vmatrix}$$

$$= -\vec{i}_r \frac{V_\varphi^2}{r} + \vec{i}_\varphi \frac{\dot{r} V_\varphi}{r} + \vec{i}_\alpha \Omega_r V_\varphi$$

Thus the acceleration is

$$\vec{A} = \frac{d\vec{V}}{dt} = \vec{i}_r \left(\ddot{r} - \frac{V_\varphi^2}{r}\right) + \vec{i}_\varphi \left(\dot{V}_\varphi + \dot{r} \frac{V_\varphi}{r}\right) + \vec{i}_\alpha V_\varphi \Omega_r \tag{32}$$

The equation of motion then can be written

$$\left.\begin{aligned} \frac{F_r}{m} &= \ddot{r} - \frac{V_\varphi^2}{r} \\ \frac{F_\varphi}{m} &= \left(\dot{V}_\varphi + \dot{r}\,\frac{V_\varphi}{r}\right) \\ \frac{F_\alpha}{m} &= V_\varphi \Omega_r \end{aligned}\right\} \tag{33}$$

subject to the kinematic equations

$$\left.\begin{aligned} \dot{\varphi} + \dot{\theta}\,\cos\,\alpha &= \frac{V_\varphi}{r} \\ \Omega_r &= \frac{\dot{\alpha}}{\cos\,\varphi} = \frac{\dot{\theta}\,\sin\,\alpha}{\sin\,\varphi} \end{aligned}\right\} \tag{34}$$

The components of the forces due to gravity including oblateness and drag in equation (33) are

$$\left.\begin{aligned} \frac{F_r}{m} &= -\frac{KM}{r^2} - \frac{6\mu KMa^2}{r^4}\,(1 - 3\,\sin^2\varphi\,\sin^2\alpha) - \frac{1}{2}\,\rho V_R \dot{r}\left(\frac{C_D A}{m}\right) \\ \frac{F_\varphi}{m} &= -\frac{12KM\mu a^2}{r^4}\,\sin\,\varphi\,\cos\,\varphi\,\sin^2\alpha - \frac{1}{2}\,\rho V_R (V_\varphi - r\Omega_e \cos\,\alpha)\left(\frac{C_D A}{m}\right) \\ \frac{F_\alpha}{m} &= -\frac{12KM\mu a^2}{r^4}\,\sin\,\varphi\,\cos\,\alpha\,\sin\,\alpha - \frac{1}{2}\,\rho V_R (r\Omega_e \sin\,\alpha\,\cos\,\varphi)\left(\frac{C_D A}{m}\right) \end{aligned}\right\} \tag{35}$$

It is noted that equations (33) and (34) are the equivalent of a set of six first-order differential equations which fully determine the history of six orbital elements for given initial conditions.

Equations of Motion in Terms of a Particular Set of Orbital Elements

There are many sets of six orbital elements, the history of which in space and time specify the path of the satellite. The set to be used depends on the problem to be studied. For instance, during circularization of the elliptical orbit, it would be reasonable to use among the orbital elements those physical quantities such as eccentricity or length of the major axis which describes the ellipse. In fact, the concept of the instantaneous ellipse to fit the trajectory at every point has been used for a long time in celestial mechanics. We will now consider the

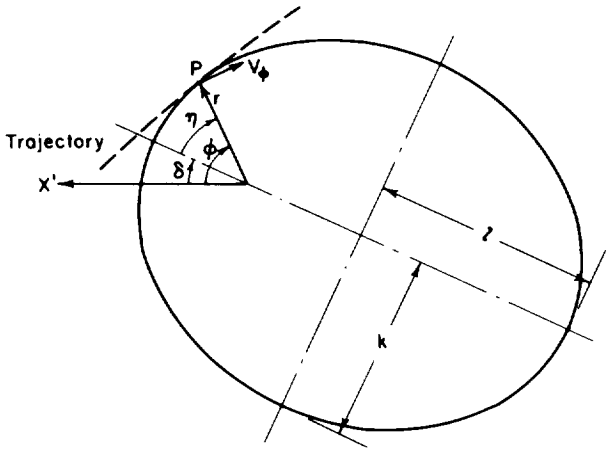

Sketch (b)

equations of motion for a special set of orbital elements based on an instantaneous-ellipse technique. This set of equations is used for certain trajectories presented herein.

The instantaneous ellipse lying in the plane of the orbit is shown in sketch (b). The ellipse is characterized by the angle δ, the eccentricity E, and the semi-major axis l. The equation of the instantaneous ellipse in polar coordinates is

$$\frac{l}{r} = \frac{1 + E\cos(\varphi - \delta)}{l(1 - E^2)} \tag{36}$$

One of the parameters of interest is the rate at which the radius vector of the elliptical path is sweeping out area. Since the rate is constant for a central force field, it should be a slowly changing function of time when drag or oblateness is included. The rate at which area is swept out is $\xi/2$, where ξ is given by

$$\xi = rV_\varphi$$

Let us now introduce two new variables specifying the value of ξ and E for the instantaneous ellipse which is to have the same value of ξ as the trajectory

$$\left.\begin{aligned} p &= \frac{\xi_o^2}{\xi^2} \\ q &= pE \end{aligned}\right\} \tag{37}$$

Here ξ_o is some reference value of ξ. Let us also introduce another constant

$$L_o = \frac{\xi_o^2}{KM} \tag{38}$$

We now wish to relate p and q to the constants of the instantaneous ellipse so that we can express r in terms of p and q. In "fitting" the instantaneous ellipse we have taken the trajectory and the ellipse at point P to have the same values of the radius vector, $\vec{r}$, and of the velocity vector, $\vec{V}$. Since the vectors $\vec{r}$ and $\vec{V}$ totally determine the dynamical state of a particle, the dynamical states are matched precisely. It follows, therefore, that the momentum and energy are also matched. The rate of sweeping for the ellipse $\xi/2$ is constant and its value is

fixed by conditions on the trajectory at P. Also, the same can be said for the sum of the potential and kinetic energies. Now the rate of sweeping out of area by the ellipse is

$$\frac{\xi}{2} = \frac{\pi k l}{T} \tag{39}$$

where k is the semiminor axis and T is the period. The period depends only on the length of the major axis

$$T = \frac{2\pi}{\sqrt{KM}} l^{3/2} \tag{40}$$

The relationship of p to the parameters of the instantaneous ellipse from equations (37), (38), (39), and (40) is

$$\frac{p}{L_o} = \frac{1}{l(1 - E^2)} \tag{41}$$

It is clear that equation (36) can now be expressed

$$\frac{l}{r} = \frac{p + q \cos \eta}{L_o} \tag{42}$$

These preceding remarks are adequate for establishing the set of variables that will now be used in the six equations of first order to describe the motion of the satellite. First we must decide on the independent variable. The variable φ is convenient if we are concerned with how quantities vary per revolution. Time as the independent variable is convenient for many other problems. With φ as the independent variable, the dependent variables are taken to be

$p = \xi_o^2/\xi^2$
$q = pE$
$\delta = \varphi - \eta$

} Parameters of instantaneous ellipse

α
θ

} Parameters specifying orientation of orbital plane

t

Equations (33) and (34) consist of a system equivalent to six first-order equations. In terms of the six preceding variables, the equations of motion given here without proof are

$$\left.\begin{aligned}
\frac{dt}{d\varphi} &= \frac{1}{\omega} \\
\frac{dp}{d\varphi} &= -\frac{2p}{\xi\omega u}\left(\frac{F_\varphi}{m}\right) \\
\frac{dq}{d\varphi} &= -\frac{dp}{d\varphi}\cos\eta + S\sin\eta \\
q\frac{d\delta}{d\varphi} &= -q\frac{d\theta}{d\varphi}\cos\alpha - \frac{dp}{d\varphi}\sin\eta - S\cos\eta \\
\frac{d\alpha}{d\varphi} &= \left(\frac{F_\alpha}{m}\right)\frac{\cos\varphi}{\omega V_\varphi} \\
\frac{d\theta}{d\varphi} &= \left(\frac{F_\alpha}{m}\right)\frac{\sin\varphi}{\omega V_\varphi \sin\alpha}
\end{aligned}\right\} \qquad (43)$$

where the quantities ω, V_φ, u, S, and η follow from the variables and from the reference quantities ξ_o and L_o:

$$\left.\begin{aligned}
\omega &= \xi u^2 - \left(\frac{F_\alpha}{m}\right)\frac{\sin\varphi\cos\alpha}{\xi u\sin\alpha} = \frac{\xi u^2}{1 + (d\theta/d\varphi)\cos\alpha} \\
\xi^2 &= \frac{\xi_o^2}{p} \\
u &= \frac{1}{r} = \frac{p + q\cos\eta}{L_o} \\
S &= \frac{1}{2p}\frac{dp}{d\varphi}q\sin\eta + \left[\frac{L_o}{\xi^2 u^2}\left(\frac{F_r}{m}\right) + p\right]\left(1 + \frac{d\theta}{d\varphi}\cos\alpha\right) \\
\eta &= \varphi - \delta \\
V_\varphi &= \frac{\xi}{r}
\end{aligned}\right\} \qquad (44)$$

Certain other identities arising in the development are also useful, especially in specifying the initial conditions:

$$\left.\begin{aligned} E &= -\frac{\xi_o^2 p(1-E^2)}{2L_o^2} = -\frac{\xi_o^2}{2L_o l} \\ \dot{r} &= \frac{\xi q \sin \eta}{L_o} \\ V^2 &= \frac{\xi^2}{L_o^2}\left(p^2 + 2pq\cos\eta + q^2\right) \\ l &= \frac{L_o}{p(1-E^2)} \end{aligned}\right\} \qquad (45)$$

During the course of the present work there appeared an English translation of a Russian paper by Taratynova, reference 1, containing equations of motion equivalent to the foregoing set. Taratynova's equations were taken from an astronomy text in Russian of 1936 vintage. His equations differ from the present ones in several particulars. First, the latus rectum and the eccentricity of the instantaneous ellipse are used instead of p and q as dependent variables. As independent variables both t and η are used. The independent variable t can be changed to φ, as in the above set of equations, simply by multiplication by ω.

It is important to inspect equation (43) for singularities arising from zeros in the denominators. Inspection shows that such zeros can conceivably arise through ω, V_φ, α, or q. From equation (44) let us write

$$\omega = \frac{V_\varphi}{r[1 + (d\theta/d\varphi)\cos\alpha]} \qquad (46)$$

It is clear that ω and V_φ both approach zero together if $d\theta/d\varphi$ is small, the only case that need concern us. If the path of the satellite is vertical in the orbital plane, ω and V_φ are zero. Equation (43) is then ill-conditioned, in the large changes in the dependent variables are accompanied by small or zero changes in the independent variable. In this instance it becomes necessary to change to a new independent variable such as the time. When α approaches zero, the orbital plane is approaching an equatorial plane. However, the zero in the denominator of the equation for $d\theta/d\varphi$ is only apparent. This is the case because F_α in the numerator, which is due to drag or the gravitational field, is proportional to $\sin\alpha$ as shown by equations (10) and (16).

The zero in the denominator of $d\delta/d\varphi$ due to q is of importance for circular orbits, as can be seen by the following expression for the eccentricity

$$E = \frac{q}{p} = \frac{qV_\varphi^2 r^2}{\xi_o^2} \qquad (47)$$

It is clear that q will be zero for circular orbits ($E = 0$) since V_φ and r are not zero. To avoid this difficulty, consider two new dependent variables to replace q

$$\left.\begin{aligned} v &\equiv q \cos \delta \\ w &\equiv q \sin \delta \end{aligned}\right\} \tag{48}$$

Then we have

$$q \cos \eta = q \cos(\varphi - \delta) = v \cos \varphi + w \sin \varphi \tag{49}$$

The differential equation for q is then replaced by the following set

$$\left.\begin{aligned} \frac{dv}{d\varphi} &= w \frac{d\theta}{d\varphi} \cos \alpha - \frac{dp}{d\varphi} \cos \varphi + S \sin \varphi \\ \frac{dw}{d\varphi} &= -v \frac{d\theta}{d\varphi} \cos \alpha - \frac{dp}{d\varphi} \sin \varphi - S \cos \varphi \end{aligned}\right\} \tag{50}$$

with

$$S = \frac{1}{2p}\left(\frac{dp}{d\varphi}\right)(v \sin \varphi - w \cos \varphi) + \left[\frac{L_o}{\xi^2 u^2}\left(\frac{Fr}{m}\right) + p\right]\left(1 + \frac{d\theta}{d\varphi} \cos \alpha\right) \tag{51}$$

It is noted that the zero in the denominator of $d\delta/d\varphi$ has now been eliminated.

The equations of Taratynova also contain a singularity. How the singularity was handled in obtaining the tabulated results given in the paper for circular orbits is not discussed.

It is clear that the system of six equalities included in equation (43) can readily be converted from φ as the independent variable to t as the independent variable. It is sufficient to invert the first equality and to multiply the next five equalities by ω.

It is possible to write the equations of motion in a form which is linear in the applied forces. In this case we also introduce the eccentricity, E, rather than q as dependent variable.

$$
\left.
\begin{aligned}
\frac{dp}{dt} &= -\frac{2rp^{3/2}}{\xi_o}\left(\frac{F_\varphi}{m}\right) \\
\frac{d\theta}{dt} &= \frac{\sin\varphi}{V_\varphi \sin\alpha}\left(\frac{F_\alpha}{m}\right) \\
\frac{d\alpha}{dt} &= \frac{\cos\varphi}{V_\varphi}\left(\frac{F_\alpha}{m}\right) \\
\frac{d\delta}{dt} &= -\frac{\sin\varphi}{V_\varphi}\operatorname{ctn}\alpha\left(\frac{F_\alpha}{m}\right) + \frac{1}{Ep}\left(1+\frac{pr}{L_o}\right)\frac{\sin\eta}{\xi}\left(\frac{\xi_o^2}{KM}\right)\left(\frac{F_\varphi}{m}\right) - \\
&\qquad \frac{\cos\eta}{Ep}\left[\frac{L_o}{\xi}\left(\frac{F_r}{m}\right) + p\xi u^2\right] \\
\frac{dE}{dt} &= -\frac{2}{\xi_o}p^{1/2}r\left[\frac{E\sin^2\eta}{2} - \cos\eta - E\right]\left(\frac{F_\varphi}{m}\right) + \\
&\qquad \frac{\sin\eta}{p}\left[\frac{L_o}{\xi}\left(\frac{F_r}{m}\right) + p\xi u^2\right] \\
\frac{d\varphi}{dt} &= \frac{V_\varphi}{r} - \frac{\sin\varphi\cos\alpha}{\xi u\sin\alpha}\left(\frac{F_\alpha}{m}\right)
\end{aligned}
\right\} \quad (52)
$$

The quantity in the square brackets represents the applied radial force less the spherical component of the gravitational field. The foregoing form of the equations of motion is convenient for deducing secular trends.

ILLUSTRATIVE EXAMPLES

The equations of motion as developed in terms of orbital elements and in geographical coordinates have their own particular uses. Two such uses will be illustrated in the present paper. In the first example we will examine the effect of the earth's oblateness and of the air drag, including atmospheric rotation, on the orbits of satellites in the equatorial plane. Such an example will use the equations of motion in terms of orbital elements. The second example in terms of geographic coordinates is concerned with the effect on the impact point of the earth's oblateness and of atmospheric rotation for nonequatorial orbits.

First Illustrative Example

As a first illustrative example, consider a satellite of given C_DA/m launched horizontally eastward on an equatorial orbit. Let the initial height about the earth be given, and let the velocity be that for a circular orbit without consideration of oblateness effects

$$(V_\varphi)_o = (V_c)_o = \sqrt{\frac{KM}{r_o}} \; ; \qquad \dot{r}_o = 0 \tag{53}$$

We will let the drag parameter C_DA/m take on values of 1 and 10. The equations of motion are then solved for four cases:

Case 1	$\mu = 0$; $\Omega_e = 0$	spherical gravitational field; nonrotating atmosphere
Case 2	$\mu \neq 0$; $\Omega_e = 0$	nonspherical gravitational field; nonrotating atmosphere
Case 3	$\mu = 0$; $\Omega_e \neq 0$	spherical gravitational field; rotating atmosphere
Case 4	$\mu \neq 0$; $\Omega_e \neq 0$	nonspherical gravitational field; rotating atmosphere

These cases permit study of the effects of oblateness and atmospheric rotation, at least for the above initial conditions.

Accuracy of calculations.- The principal factors influencing the accuracy of the calculated results are the interval size and the number of significant figures carried in the calculations. Eight significant figures are carried throughout. The density was obtained by exponential interpolation in the ARDC density table and is not accurate to eight significant figures, although the density calculations repeat consistently to eight figures. With respect to interval size, the results of interval sizes in $\Delta\varphi$ of $\pi/8$ and $\pi/32$ are shown in the following list. This list gives certain quantities as calculated at $\varphi = 13\pi$ for $C_DA/m = 1$, case 1, initial altitude 120 miles:

	$\Delta\varphi = \pi/8$ radians	$\Delta\varphi = \pi/32$ radians
ξ, ft^2/sec	55.084587×10^{10}	55.084366×10^{10}
v	0.21953070×10^{-7}	0.23739280×10^{-7}
w	-0.12332460×10^{-4}	-0.12347577×10^{-4}
t, sec	34452.440	34452.110
r, ft	21554337	21554164
$\dot{r}$, ft/sec	-0.32462706	-0.32502373
λ, radians	40.840698	40.840779
E	0.12702521×10^{-4}	0.12717994×10^{-4}
V_φ, ft/sec	25556.150	25556.253
$\ddot{r}$, ft/sec^2	-0.68629226×10^{-6}	-0.71082937×10^{-6}
h, ft	627909.00	627736.00
p	0.97086900	0.97087600

The quantities are sufficiently close for most engineering purposes. Note that the altitude difference is 173 feet, which represents about a 0.03-percent error. Similar calculations were performed for case 2 with the same general results. On the basis of these results, it was decided to use $\pi/8$ as the basic interval for the calculations.

Periodic variations.- In figure 3(a) are plotted the altitude and eccentricity variations for one period for $C_DA/m = 1$, cases 1 and 3. The loss in altitude with atmospheric rotation is slightly less than without rotation because the dynamic pressure and hence drag is decreased about 12 percent by rotation for eastward launchings. The path is a spiral for which the eccentricity, although small, has a strong periodic component.

The principal effects of oblateness during a revolution are illustrated by comparison of figures 3(a) and 3(c). The differences in the scales of the ordinates should be noted during the comparison. Thus the effect of atmospheric rotation is evident in figure 3(a) but not in 3(c). It is of interest that the altitude difference during one revolution is about 66,000 feet with oblateness, compared to about 800 feet without it. To explain this oblateness effect, we make use of the full gravitational field for an equatorial orbit as given by equation (10)

$$\frac{G_r}{m} = -\frac{KM}{r^2}\left(1 + 6\mu\,\frac{a^2}{r^2}\right) \tag{54}$$

The gravitational field is increased by 6μ, or about 0.16 percent. Since the satellite was initially in an equilibrium circular orbit with $\mu = 0$, suddenly "turning on" the oblateness at the initial altitude leaves the satellite with a velocity deficiency, just as if a tangential retrorocket had been fired. Since $\dot{r}_o = 0$, the satellite location immediately turns into an apogee point; and, neglecting drag, the path becomes elliptical. From an energy consideration, neglecting drag, it is shown in appendix C that the altitude difference between perigee and apogee is

$$r_a - r_p = 2r_a\epsilon \; ; \qquad \epsilon = 6\mu\,\frac{a^2}{r^2} \tag{55}$$

We find that oblateness for equatorial orbits thus causes a difference in altitude between apogee and perigee of $r_a - r_p = 66{,}700$ feet. Without oblateness but with drag figure 3(a) shows an altitude loss for half a revolution of about 400 feet. The difference in altitude between perigee and apogee is almost exclusively due to oblateness for the present value of C_DA/m. In fact the calculated value from equation (55) of 66,700 feet for oblateness alone is in very good accord with the value from the complete calculations of 67,081 feet for the combined effects of oblateness and drag. It is also clear that the approximate figure of 67,000 feet is not sensitive to initial altitude since drag is not significant and the oblateness effect as calculated from equation (55) is insensitive to changes in altitude for near satellites. With regard

to the net loss of altitude per revolution, oblateness has the effect in the present case of doubling this loss. This specific result applies to the altitude range for which $d(\log \rho)/dh$ is the same as for the present example.

For C_DA/m of 10, the altitude changes and the eccentricity are about 10 times those for $C_DA/m = 1$, but there are no qualitative differences. The effect of the rotation of the atmosphere has a small effect in all cases.

Secular trends; limitations of calculation.- The manner in which the altitude and eccentricity vary from revolution to revolution, the secular trends, is illustrated in figure 4. For the range of figure 4(a) the decrease in altitude per revolution is a nearly linear function of the number of revolutions. However, for C_DA/m of 10, figure 4(b), the rate of decrease of altitude becomes greater at lower altitudes since large density increases occur. While the altitude variations are as we would expect, the secular variations in eccentricity are of particular importance. For C_DA/m of 1, figure 4(a) shows the eccentricity variation for 2 cycles, and then continues the envelope for 10 cycles, the limit of the calculation. However, for C_DA/m of 10, the eccentricity shows a divergence in the range of calculations, and the calculations in fact break down.

To see how the calculations break down, let us examine the variation of eccentricity with φ as shown in figure 5. (For the equatorial orbit being considered φ and λ differ only slightly.) Actually the oscillatory variation in E is no longer significant, as in figure 4(b), but E has what appears to be a nearly vertical tangent. The instantaneous ellipse is therefore undergoing very rapid changes in eccentricity. The interval size is too coarse to follow the rapidly changing curvature. By reducing the interval size, and increasing the number of figures carried in the calculation, the range of the calculations can be increased. However, this method is inherently unsuited to calculation of the terminal phase of the trajectory for the following reasons: In the terminal phase of the trajectory the satellite descends vertically or nearly vertically along a radius vector. For such motion there is little or no change in φ, the independent variable. Therefore, a better-conditioned independent variable, such as time, should be used.

Regression of line of nodes and movement of line of apsides.- The solutions for the movement of the line of nodes and the motion of the line of apsides for the case of oblateness but no drag are known. The variation in these quantities per revolution can be obtained by integrating the equations for $d\theta/d\varphi$ and $d\delta/d\varphi$ from $\varphi = 0$ to 2π on the basis that departures from the basic ellipse are small. The following results are taken from reference 13.

$$\left.\begin{aligned} \Delta\theta &= -12\pi\mu\left(\frac{a}{r}\right)^2\left(\frac{V_c}{V_\varphi}\right)^4 \cos\alpha \\ \Delta\delta &= 6\pi\mu\left(\frac{a}{r}\right)^2\left(\frac{V_c}{V_\varphi}\right)^4 (4 - 5\sin^2\alpha) \end{aligned}\right\} \qquad (56)$$

where V_c is the circular orbital speed at radius r for no oblateness (eq. (53)). It is to be noted that the first equation, strictly speaking, applies to the secular change for one nodal period,[4] that is, for the time to go from one ascending node to the next. It happens that drag forces, being in the plane of the orbit, have only a very small influence on the regression of the line of nodes, as shown by the following list.

	θ, radians		
$\frac{\varphi}{2\pi}$	$\frac{C_D A}{m} = 1$; case 2	$\frac{C_D A}{m} = 10$; case 2	Equation (56)
1	-0.009689	-0.009695	-0.009696
2	-.01938	-.01941	-.01939
3	-.02907	-.02914	-.02909
4	-.03876	-.03892	-.03878

The movement of the line of apsides (the major axis of the instantaneous ellipse) is vitally influenced by the drag. It is first desirable to note what happens in the absence of drag for an equatorial orbit. The line of nodes, which can be visualized only for orbital planes away from the equatorial plane, moves backward against the motion of the satellite at 0.555° per revolution. The corresponding rate for the moon is about 1.5° per revolution. The line of apsides moves forward in the direction of the satellite at twice this rate. As a result, the line of apsides moves around the equator with respect to an inertial framework at precisely the same rate that the line of nodes moves backward.

With the introduction of drag the line of apsides tends to move around the orbit with variable lag, at the average speed of the satellite. To show clearly the motion of the line of apsides consider the angle δ given by equation (48)

$$\delta = \tan^{-1}\frac{w}{v} \qquad (57)$$

The angle δ gives the position of perigee[5] measured from the line of nodes. A plot of w versus v shown in figure 6(a) illustrates how δ starts out at π for $\varphi = 0$ for the case shown and increases steadily thereafter. If δ leads or lags φ by a constant amount at all times,

[4]The nodal period is sometimes referred to as the synodic period.

[5]The position of perigee is sometimes referred to as the minor apsis.

then a curve of $(\delta - \varphi)$ versus φ would be a straight line. The parameter $(\delta - \varphi)/2\pi$ is shown versus $\varphi/2\pi$ in figure 6(b) for the present case. The variable lead of δ over φ approaches $\pi/2$ after several revolutions. The principal conclusion to be drawn from these results is that the very small motions of the line of apsides due to oblateness alone are completely masked when drag is included because the line of apsides moves with average speed of the satellite. The concept of the line of apsides becomes useful now as a measure of lead or lag of the angular position of the major axis of the instantaneous ellipse from the angular position of the satellite.

Second Illustrative Example

As a second illustrative example, consider a satellite launched from the equator in an orbital plane inclined at 65° to the equatorial plane. The initial height above the equator is taken as 80 miles, and the satellite is launched at circular orbital speed. The initial altitude was chosen low enough to obtain impact in about a revolution or less. The launching velocity was not always horizontal as in the previous example, but radial velocities were introduced as follows: $\dot{r}_o/(V_\varphi)_o = 0, -0.01, -0.05, -0.10$. Values of $C_D A/m$ of 1 and 10 are included. The equations of motion were integrated numerically for the four cases considered in the first illustrative example. An attempt was made to carry all cases to impact. Impact altitude is taken to correspond to 1000 feet altitude. The calculations have been made using geographic coordinates, but were checked against calculations in one case using the elliptic orbital elements method.

Accuracy of calculations.- The accuracy of the calculated results in this example can be assessed by several means. First, we can compare calculations on the basis of geographic coordirates with those on the basis of elliptic orbital elements. We can also vary the time interval used in the calculations based on geographic coordinates. Pursuing the first comparison, consider a satellite with $C_D A/m = 1$, $\dot{r}_o/(V_\varphi)_o = 0$, case 1, for $\varphi = 6.037$ radians. The orbital quantities for these conditions are compared in the following list.

12-4-58A

	Orbital elements, $\Delta\varphi = \pi/64$ radians	Geographic coordinates, $\Delta t = 30$ seconds
φ, radians	6.0377500	6.0377582
v	-0.0038107764	-0.0038172179
w	0.0030982814	0.0031003921
t, sec	5010.6056	5010.6056
r, ft	2.1258168×10^{7}	2.1258139×10^{7}
$\dot{r}$, ft/sec	-54.238659	-54.265940
λ, radians	6.1777185	6.1777180
E	0.0049667594	0.0049733320
V_φ, ft/sec	2.5675599×10^{4}	2.5675529×10^{4}
$\ddot{r}$, ft/sec^2	-0.13947319	
h, ft	0.335174×10^{6}	0.335146×10^{6}
p		0.98883584
ψ, radians	-0.22203323	-0.22202809
α, radians	1.1344640	1.1344641

It is noted that the two sets of calculations are in good agreement, indicating that no gross mistakes have occurred either in analysis or calculation. The interval size for the orbital elements is the 128th part of a revolution, while that for the geographic coordinates is essentially the 180th part of a revolution.

The foregoing comparison is made for a satellite descending from 80 miles altitude to about 63 miles altitude in one revolution. When the calculations were performed with the 30-second interval, it became clear on numerical grounds after some point in time that the interval size was too large. All calculative cases using a 30-second interval exhibited this behavior before impact. Thus while an interval size of 30 seconds is satisfactory for the initial phase of the trajectory, it is not adequate for the terminal phase. Some time before the calculations exhibited inaccuracies with the 30-second interval, the interval was switched to 3 seconds. The calculations were then continued to impact.

Let us now compare the trajectories calculated using the foregoing method based on two interval sizes with the trajectory calculated using a 3-second interval size all the way. Since we are principally interested in the point of impact, the following comparison yields a good idea of how accurate the point of impact is. The example considered for this comparison corresponds to $C_DA/m = 1$, case 1, $\dot{r}_o/(V_\varphi)_o = 0$. In the left-hand column a 3-second interval was used to compute the trajectory all the way to the point of impact. In the right-hand column, the 30-second interval was used to t = 5760 seconds and the 3-second interval from then until impact at 5991 seconds.

Interval size, sec	3 only	30 and 3
t, sec	5991	5991
cos φ	0.86217703	0.86456735
$\dot{r}$, ft/sec	166.43243	167.09205
λ, radians	6.5265953	6.5241574
V_φ, ft/sec	0	0
h, ft	327	592
ψ, radians	0.47702802	0.47302309

In this case the satellite travels slightly more than a complete revolution around the world. The difference in latitude at the end of 5991 seconds is 15.87 miles and the difference in longitude is 8.58 miles. Since the range is over 25,000 miles, these accuracies for the impact point were considered satisfactory. Hence most of the calculations were made on the basis of a 30-second interval followed by a 3-second interval in the terminal phase.

General features of the trajectories.- To show the general features of the trajectories, consider figures 7(a), 7(b), and 7(c) constructed for $C_DA/m = 1$, $\dot{r}_o/(V_\varphi)_o = 0$. The altitude variations with time shown in figure 7(a) exhibit several important effects. The general waviness is due to the nonspherical figure of the earth. At $t = 0$ the satellite starts at the equator, and at about 1200 seconds the satellite reaches its maximum north latitude for which the earth radius is least for the orbit and the altitude is correspondingly greater. Subsequent passes over the equator through maximum and minimum latitude cause further bumps. In the cases including the gravitational effects of oblateness, the time of flight is significantly shorter than without oblateness effects. The basic reason for this behavior has already been discussed in connection with the equatorial orbits. Oblateness causes the satellite to descend lower into the atmosphere. The resulting higher drag thus reduces the flight time as shown.

The latitude-longitude variations of the satellite for the four cases are given in figure 7(b). The paths for the four cases are essentially the same until the time atmospheric drag initiates entry. At this time the latitude and longitude are essentially frozen. What this means generally is that at a given time the satellite for the four different cases has nearly the latitude and longitude given by the Keplerian solution, but the altitudes differ significantly. As a result, for the four different cases the satellite enters the final constant longitude-latitude phase at different times.

During the first part of the trajectory the satellite not only follows the same latitude-longitude path for all four cases, but it also appears at a given longitude and latitude at the same time. However, near the very end of the trajectory the satellite decelerates rapidly just prior to turning down into the atmosphere. During this phase the

satellite appears at a given latitude and longitude somewhat later than for those cases for which the satellite has a greater altitude. Included on the curves of figure 7(a) are ticks which indicate where the eccentricity nearly reaches unity. These ticks correlate closely with the position where the latitude and longitude become constant.

The eccentricity variations of figure 7(c) shed some light on the motion. The eccentricity started at zero because of the particular initial conditions taken in the present calculation; namely, those corresponding to a circular satellite orbit (see eq. (B11)). The eccentricity remains small for the first part of the trajectory and shows characteristic waviness because of the nonspherical figure of the earth. During the final half of the trajectory the eccentricity rapidly rises nearly to unity and remains there during the terminal phase. The value of unity is associated with a vertical path as shown by equation (B7). For cases 1 and 2 the eccentricity remains essentially unity until impact, in most instances. In other instances, however, the machine calculation of eccentricity becomes erratic. Actually, for a vertical path the eccentricity is a derived quantity which has no particular significance, so that the erratic behavior of E does not reflect on the accuracy of the trajectory calculations.

Impact point.- The calculations of this illustrative example also shed some light on how the oblateness component of gravitational field influences the impact point, as well as how atmospheric rotation influences it. Let $\psi_1, \lambda_1; \psi_2, \lambda_2; \psi_3, \lambda_3; \psi_4, \lambda_4$ be the impact coordinates for cases 1, 2, 3, and 4, respectively. Then the effects of oblateness on the impact point with no atmospheric rotation are $\psi_2 - \psi_1, \lambda_2 - \lambda_1$ and with atmospheric rotation are $\psi_4 - \psi_3, \lambda_4 - \lambda_3$. These quantities are tabulated in table I as a decimal part of the total range from the assumed initial point to impact. The coordinates λ_4, ψ_4 of the impact point are also tabulated together with the great circle distance, s, between 0, 0 and λ_4, ψ_4. These latter quantities as calculated in radians were multiplied by a, the equatorial radius, to convert to miles. The ranges are as measured in the inertial system XYZ and are not those for an observer on the earth. The earth ranges can be determined with the help of the tabulated flight times. The first important point is that oblateness causes large percentage errors in range for re-entry at zero or very small angles. These errors are simply the calculated differences in impact point between those for μ equal to zero and for μ not equal to zero. As previously mentioned, the initial velocity is too low to launch the satellite into a circular orbit when μ is not zero.

In the foregoing discussion the effects of oblateness have been taken as differences in the calculated results due to neglecting the oblateness gravitational terms in the equations of motion for the same initial conditions. It appears desirable to take some account of oblateness in the initial conditions. For equatorial orbits this is easily accomplished by making V_φ equal to that for a circular orbit. Without

oblateness the value of V_φ to achieve a circular orbit is V_c, but with oblateness the initial V_φ should be

$$V_\varphi = V_{co} = \sqrt{\frac{KM}{r}\left(1 + \frac{6\mu a^2}{r^2}\right)}$$

Let us now differentiate the following three examples:

Example	Initial V_φ	μ in equations of motion
A	$V_\varphi = V_c$	Not included
B	$V_\varphi = V_c$	Included
C	$V_\varphi = V_{co}$	Included

For these three examples trajectories were computed to impact for the following initial conditions:

$$\alpha_o = 0^\circ;\ h_o = 80 \text{ miles};\ C_DA/m = 1;$$

$$\dot{r}_o = 0;\ \theta_o = \lambda_o = \psi_o = 0^\circ$$

The following results were obtained:

	Example A	Example B	Example C
h, ft	151	270	193
t, sec	4,058	2,742	4,017
V_φ, ft/sec	10^{-11}	10^{-10}	10^{-10}
$\dot{r}$, ft/sec	165.883	166.310	166.121
λ, radians	4.4820	2.9011	4.4338
λ or s, miles	17,750	11,498	17,570

The foregoing results are as one might anticipate. For $V_\varphi = V_c$ the range is reduced 6,252 miles by including oblateness in the equations of motion, but with $V_\varphi = V_{co}$ the range is reduced only 180 miles.

If the inclination of the orbital plane to the equator is changed from zero, a purely circular orbit with oblateness is not possible. As a matter of curiosity the value of V_φ for a nonequatorial orbit was changed from V_c to V_{co} to see how the range was affected. The case investigated corresponds to $\alpha_o = 65^\circ$, $C_DA/m = 1$, $\dot{r}_o = 0$, and $h_o = 80$ miles. The ranges are tabulated for the same conditions as examples A, B, and C.

Example A; s = 26,987 miles

Example B; s = 18,736 miles

Example C; s = 38,126 miles

The ranges are great circle ranges. It is noted that including μ in the equations of motion but not adjusting the initial value of V_φ reduces the range by about 30 percent. If the initial value of V_φ is boosted to V_{co}, the range is greatly increased for the present orbit even though μ is included in the equations of motion.

It is clear that for the present initial conditions increasing C_DA/m from 1 to 10 diminishes the effect of oblateness on impact point. This result is in accordance with the fact that increasing C_DA/m decreases the importance of gravitational forces compared to drag forces. Increasing the initial downward velocity also decreases the proportionate error in impact point. This effect is similar to decrease in miss distance due to errors in launching speed as the downward launch angle is increased.

For manned re-entry for which C_DA/m is of the order unity and the entry angle is of the order of a degree or less ($\dot{r}/V_\varphi \leq -0.02$) to limit normal accleration, oblateness has an influence of several hundred miles in latitude and longitude on the point of impact. Including or neglecting atmospheric rotation does not significantly influence this result.

The influence of atmospheric rotation on the impact point is generally not so large as that of oblateness. The influence of atmospheric rotation is represented by $\psi_3 - \psi_1$, $\lambda_3 - \lambda_1$, or $\psi_4 - \psi_2$, $\lambda_4 - \lambda_2$. These quantities are tabulated in table II in the same manner as table I.

As the downward launch angle is increased, the percentage effect of atmospheric rotation on range generally increases. Such an effect is due to the fact that the satellite spends more of its time in the lower atmosphere where the air density is higher. Also, as C_DA/m is increased, the drag due to atmospheric rotation assumes more importance and increases the effect of atmospheric rotation on impact point. As the satellite approaches its impact point, its vertical velocity usually is small compared to the rotational speed of the atmosphere. The atmosphere thus drags the satellite around with it at constant ψ and increasing λ. As seen by the observer on the earth, the satellite would descend vertically except for a small slippage between the satellite and the atmosphere. For a value of C_DA/m of 1 and for $\dot{r}_o/(V_\varphi)_o$ of -0.01, such as might be used for manned entry, a 150-mile change in impact point is due to atmospheric rotation for the present initial conditions.

RELATIVE IMPORTANCE OF VARIOUS TERMS IN EQUATIONS OF MOTION

From the complete trajectories presented in the previous calculated examples, it is possible to examine the order of magnitude of the various terms occurring in the equations of radial and tangential motion. The resulting information will show what physical terms are important for various phases of the trajectory and, hence, will suggest simplifications permissible for analytical work in particular. Also, the information will show where in the trajectory the assumption stated in equation (3) becomes valid; that is, where the entry or terminal phase begins and hence where the solution of Chapman (ref. 4) is valid.

The parameter which has particular significance for dividing the trajectory into various phases is the ratio of tangential velocity V_φ to circular satellite velocity V_c. To obtain a number whose logarithm is not $-\infty$ when $V_\varphi = 0$, let us use $1 - V_\varphi/V_c$ as the parameter. In figure 8(a) the variations with $1 - V_\varphi/V_c$ are shown of the terms in the tangential equation of motion

$$\dot{V}_\varphi + \frac{\dot{r}V_\varphi}{r} = \frac{D_\varphi}{m} + \frac{G_\varphi}{m} \tag{58}$$

The term $\dot{r}V_\varphi/r$ is less than 10 percent of $\dot{V}_\varphi$ when V_φ is less than about 99-percent V_c. This result gives a quantitative measure of when the assumption of equation (3) is met. Figure 8(b) was constructed to show that the figure of 99 percent does not change when the drag parameter C_DA/m is increased from unity to 10.

Figure 8(b) exhibits phenomena not manifest in the range of figure 8(a). First it is seen that Keplerian motion characterized by $\dot{V}_\varphi = -\dot{r}V_\varphi/r$ is never realized for this example. The sequence of events is interesting to examine. At time zero the drag is in equilibrium with the tangential acceleration force and the satellite slows down. However, although drag initially makes $\dot{V}_\varphi$ negative, the satellite tends to speed up as it drops in altitude until $\dot{V}_\varphi$ is zero. At this point the drag is in equilibrium with the acceleration force due to $\dot{r}V_\varphi/r$. The satellite speeds up as it drops in altitude until a maximum value of V_φ is reached, when $\dot{V}_\varphi$ is again zero. Thereafter the satellite decelerates tangentially at an increasing rate, and the motion is in accord with the solution of Chapman. For $C_DA/m = 1$ figure 8(b) shows that setting $\dot{r}_o = -0.1(V_\varphi)_o$ does not alter the range of applicability of Chapman's assumption.

With regard to the equation of radial motion

$$\ddot{r} - \frac{V_\varphi^2}{r} = \frac{D_r}{m} + \frac{G_r}{m} \tag{59}$$

the magnitudes of the four terms are shown in figure 9(a) for C_DA/m of unity and $\dot{r}_o$ of zero. It is interesting to note that the gravitational and centrifugal forces are in balance until V_φ is about 0.9 V_c. There is then an interval where four terms are important. For V_φ near zero, the drag and gravitational terms are nearly in balance. However, the radial acceleration term $\ddot{r}$ cannot be ignored if accurate terminal velocities are desired, since it is about 30 percent of the other two terms. If C_DA/m is increased to 10 from unity (fig. 9(b)), or if the initial launch angle is 0.1 radian downward (fig. 9(c)), the radial acceleration still cannot be neglected except for rough calculations.

A patching technique is useful to establish a rough complete trajectory. For V_φ above about 0.99 V_c the trajectory can be approximated by the method of appendix A. For V_φ equal to about 0.99 V_c the solution can be joined to that of Chapman, as described in reference 4, and continued down to the point where the flight path is nearly vertical. Although the equation of Chapman is still valid for vertical flight, the numerical solution of his equation loses accuracy because of a singularity. A solution for the vertical part of the trajectory is given in reference 14.

Let us examine the contribution of atmospheric rotation to the drag term since this has important implications concerning the adequacy of approximate two-dimensional theories which usually neglect atmospheric rotation. This question assumes significance in the terminal phase of the trajectory. Let us examine the flight path angles as seen by an observer in an inertial framework and by an observer on the earth. The flight path angle in the inertial framework is simply given by

$$\tan \gamma_i = \frac{\dot{r}}{V_\varphi}$$

For an earth observer, $\dot{r}$ is unchanged but V_φ is decreased for eastward motion by the component of the earth's rotational speed in the orbital plane. This component of speed is $r \cos \psi \Omega_e \sin \beta$ or $r\Omega_e \cos \alpha$. The flight path angle, γ_e, as seen by an earth observer is simply given by

$$\tan \gamma_e = \frac{\dot{r}}{V_\varphi - r\Omega_e \cos \alpha}$$

To illustrate the influence of earth rotation and observational position on flight path angle, figure 10 has been prepared. The initial conditions are taken to be

$$\alpha_o = 65^\circ;\ (V_\varphi)_o = (V_c)_o;\ \dot{r}_o = 0;\ h_o = 80 \text{ miles};$$

$$C_DA/m = 1;\ \theta_o = \lambda_o = \psi_o = 0^\circ$$

The first curve to which attention is called is the plot of γ_i for case 1, $\mu = 0$, and $\Omega_e = 0$. As the satellite approaches impact for this case, the flight path approaches a nearly vertical condition as seen by

an observer in the inertial framework. If we now include atmospheric rotation, (and oblateness), the variation of γ_i for case 4 is obtained as shown. The behavior of γ_i in this case is distinctly different since it now reaches a maximum near 30° and rapidly decreases thereafter. What has occurred in the terminal phase is that the radial speed has been reduced to several hundred miles per hour by air drag, but the horizontal speed V_φ has been increased to a much greater value by atmospheric rotation. The atmospheric rotation causes the trajectory to curve almost directly eastward at constant latitude ψ with a horizontal speed equal very nearly to $r\Omega_e \cos \psi$. At the equator this speed is about 6 percent circular orbital speed for near earth satellites. Thus, approaching impact, the satellite has a nearly constant value of V_φ/V_c less than 0.06.

The distinctly different characteristics of the trajectory in the terminal phase with and without atmospheric rotation raise the important point whether two-dimensional theories neglecting atmospheric rotation are really applicable to the terminal phase. The question can be answered in the affirmative provided the correct interpretation is given to the two-dimensional theories. In this connection the flight path angle as seen by an earth observer has been plotted in figure 10 for case 4 which includes oblateness and rotation. Not unexpectedly, it turns out to be in close accord with γ_i for case 1, no oblateness or rotation. The following interpretation is given to this result: Two-dimensional theories neglecting atmospheric rotation (but including drag) yield trajectories which tend to be nearly vertical in the terminal phase provided $C_D A/m$ is not too small compared to unity. These theories can be applied with good accuracy to three-dimensional trajectories including atmospheric rotation if the results are interpreted to apply to the motion as seen by an earth observer. In fact, with this interpretation it would be a mistake to include atmospheric rotation in the two-dimensional theory.

COMPARISON OF EQUATORIAL TRAJECTORY WITH TRAJECTORIES OF APPROXIMATE TWO-DIMENSIONAL THEORIES

It is of interest to compare approximate two-dimensional analytical results with an equatorial trajectory as calculated numerically by the present method. For this reason a special equatorial trajectory was computed neglecting atmospheric rotation and oblateness effects, factors not usually considered in two-dimensional theories. The initial conditions for the trajectory are

$$h_o = 80 \text{ miles}; \quad (V_\varphi)_o = (V_c)_o; \quad \dot{r}_o = 0;$$

$$\theta_o = \lambda_o = \psi_o = \alpha_o = 0^\circ$$

The trajectory was calculated for a 1-second interval using geographic coordinates. The values of various quantities during re-entry are listed in table III.

The approximate theories compared with the present method include that of appendix A, the method of Chapman (ref. 4), and an extension of the results of Linnell (ref. 14). These theories are applied, respectively, to the initial part of the flight, the middle part of the flight, and the terminal phase of the flight.

12-4-58A

Let us first consider that part of the flight from V_φ/V_c from about 1.000 to about 0.995, during which most of the range occurs. The small variations in V_φ and r permit the simple approximate solution of appendix A. The variations of h and $\dot{r}$ with t obtained by this method are compared in figure 11 with those given in the foregoing table. Solutions are given for two time intervals in the calculation, a short interval and a long interval as described in appendix A. For the short time interval the values of $\dot{r}$ and h are in fair accord with the tabulated values out to larger values of t than for the longer time interval.

Consider now the phase of the trajectory with V_φ less than 99.5-percent circular orbital speed. This is the region where the $\dot{r}V_\varphi/r$ force is negligible and the solution of Chapman applies. This solution is expressed in the form of a parameter Z tabulated as a function of $\bar{u}$

$$\left.\begin{aligned} Z &= \frac{1}{2}\left(\frac{C_D A}{m}\right)\bar{u}\rho\sqrt{\frac{r}{\beta}} \\ Z' &= -\sqrt{\beta r}\,\sin\gamma + \frac{Z}{\bar{u}} \\ \bar{u} &= \frac{V_\varphi}{V_c} \end{aligned}\right\} \qquad (60)$$

The Chapman solution considered here is that for $\bar{u} = 0.995$ and $\gamma = -0.5^\circ$, and is the available one most nearly approximating the present calculations. For the initial values of $\bar{u}$ and γ, the solution of Chapman gives a value for Z. From this initial value of Z and the value of $C_D A/m$ of unity, the initial value of the density can be calculated from equation (60). The values of h, $\dot{r}$, V_φ, and λ are compared in figure 12(a) and the value of γ is compared in figure 12(b). The initial altitude obtained from the Chapman solution is slightly less than that obtained from the present solution. Some of this difference is due to the slight differences in γ exhibited in figure 12(b). Generally speaking, the solutions are in good accord. The tendency of the solutions for γ, V_φ, and h to interlace is probably due to slight differences in the atmospheric altitude-density relationships assumed in the two methods. Chapman has used an exponential atmosphere in his work, while the present work is based on the ARDC atmosphere.

In the terminal phase, the present tabulated solutions of Chapman do not continue entirely to impact but stop at a value of $\bar{u} = 0.025$. For $\bar{u} = 0$, vertical flight, the solution of Linnell, reference 14, is

available. In an unpublished investigation Elliott D. Katzen of Ames Laboratory has adapted the solution of Linnell to slight departures from vertical flight. His calculated values for $\bar{u}$ less than 0.025 agree well with the present values.

CONCLUDING REMARKS

The principal purpose of this paper has been accomplished; namely, to present equations for calculating complete trajectories of earth satellites from outer space to the ground under the influence of air drag and gravity, including oblateness[6] and to apply these to several cases of entry from circular orbits.

Equations of motion based on an "instantaneous ellipse" technique, with polar angle as the independent variable, were found suitable for automatic computation of orbits in which the trajectory consists of a number of revolutions. This method is suitable as long as the satellite does not enter the terminal phase. In the terminal phase of the trajectory, equations of motion in spherical polar coordinates with time as the independent variable were found to be suitable.

In the first illustrative example, the effects of the oblateness component of the earth's gravitational field and of atmospheric rotation were studied for equatorial orbits. The satellites were launched into circular orbits at a height of 120 miles, an altitude sufficiently high that a number of revolutions could be studied. The importance of the oblateness component of the earth's gravitational field is shown by the fact that a satellite launched at circular orbital speed, neglecting oblateness, has a perigee some 67,000 feet lower when oblateness forces are included in the equations of motion than when they are not included. Also the loss in altitude per revolution is double that of a satellite following an orbit not subject to oblateness. The effect of atmospheric rotation on the loss of altitude per revolution was small. As might be surmised, the regression of the line of nodes as predicted by celestial mechanics, equation (56), is unchanged when drag is included. It is clear that the inclination of the orbital plane to the equator will be relatively unaffected by drag for no atmospheric rotation since the drag lies in the orbital plane in this case. With the inclusion of atmospheric rotation it was found that the inclination of the plane changed about 10^{-6} radians per revolution. Thus the prediction of the position of the orbital plane of an earth satellite is not complicated by the introduction of drag. The line of apsides, which without drag but with oblateness moves slowly in space, tends to move with the satellite when drag is included in the calculations. As a result the usual linearized solutions based on oblateness alone must be basically altered when drag is included to take into account the rapid movement of the line of apsides.

---

[6]No attempt was made herein to take into account gravitational anomalies or surface cross winds.

In the second illustrative example, the final revolution was calculated to impact for a number of trajectories in an orbital plane inclined at 65° to the equator. Of particular interest are the large effects that the oblateness gravitational field and atmospheric rotation have on the impact point. For a value of C_DA/m of unity, and for an initial downward angle at 80-miles altitude of 0.01 radian, such as might be utilized for manned re-entry, oblateness had an influence of about 300 miles in the impact point, and atmospheric rotation had about a 150-mile influence.

From the complete trajectories calculated automatically, it was possible to examine the relative importance of the various terms in the equations of motion. For the equation of tangential motion, the term proportional to $\dot{r}V_\varphi/r$ is negligible, as long as the local value of V_φ is less than 99 percent of V_c. This result indicates that for V_φ less than 0.99 V_c the equation of Chapman (ref. 4) can be used. For the equation of radial motion, the radial component of gravity and the centrifugal force dominate the motion for values of V_φ near V_c. However, for $V_\varphi \ll V_c$, where the trajectory is nearly vertical, the radial component of gravity and the drag dominate the radial motion, but the radial acceleration is not generally negligible.

It was found that two-dimensional solutions neglecting atmospheric rotation can be used to approximate three-dimensional solutions with atmospheric rotation. In this connection, two-dimensional theories must be interpreted as being viewed by an observer on a rotating earth.

Several gaps exist in the solutions available for studying the dynamics of earth satellites. First, to the authors' knowledge, no linearized theory exists for predicting the periodic variation of the elliptic elements during circularization of the ellipse or during spiral decay, taking into account drag. This linearized solution would have to take into account the fact that the line of apsides tends to move with the satellite. Second, a missing ingredient in the accurate automatic computation of impact points is precise knowledge of the variation in atmospheric density with latitude, season, or time of day.

Ames Research Center
National Aeronautics and Space Administration
Moffett Field, Calif., July 15, 1958

APPENDIX A

APPROXIMATE SOLUTION FOR TWO-DIMENSIONAL TRAJECTORIES NEAR CIRCULAR ORBITAL SPEED TOGETHER WITH NUMERICAL EXAMPLE

Since a considerable part of the range of a satellite re-entering the atmosphere is traversed at a tangential speed V_φ nearly equal to circular orbital speed, it would be helpful to have an approximate solution for this case. In what follows we assume that the percentage changes in V_φ and r are small, but the percentage change in air density ρ may be large. We will find an approximate solution $r = r(t)$ subject to the initial conditions $r = r_o$, $\dot{r} = \dot{r}_o$ at $t = 0$. (The initial value of $\ddot{r}_o$ can be calculated from $\dot{r}_o$ and r_o.)

Consider the equations of motion in the following form:

$$\left.\begin{aligned} \ddot{r} - \frac{V_\varphi^2}{r} &= \frac{D_r}{m} + \frac{G_r}{m} \\ \dot{V}_\varphi + \dot{r}\,\frac{V_\varphi}{r} &= \frac{D_\varphi}{m} + \frac{G_\varphi}{m} \end{aligned}\right\} \qquad \text{(A1)}$$

If we neglect oblateness, then G_φ is zero. Also, the flight path angle is nearly zero so that D_r can be neglected as shown in figure 9. The equations of motion with no atmospheric rotation are

$$\left.\begin{aligned} \ddot{r} &= \frac{V_\varphi^2}{r} - \frac{KM}{r^2} \\ \dot{V}_\varphi r + \dot{r}V_\varphi &= -\frac{1}{2}\,\rho V_\varphi^2 r\left(\frac{C_D A}{m}\right) \end{aligned}\right\} \qquad \text{(A2)}$$

Since the only variable in the tangential equation of motion with any appreciable percentage change is ρ, we can integrate the equation as follows

$$(rV_\varphi) = (rV_\varphi)_o - \frac{1}{2}\,\overline{\rho} V_\varphi^2 r\left(\frac{C_D A}{m}\right)t \qquad \text{(A3)}$$

The quantity $\overline{\rho}$ is the mean density during the time interval between $t = 0$ and $t = t$, and $(rV_\varphi)_o$ is evaluated at $t = 0$. Equation (A3) gives the time range of change of area sweeping. Since V_φ and r are slowly varying functions of time, the product rV_φ also is.

To obtain the altitude as a function of time necessitates an integration of the radial equation of motion

$$\ddot{r} = - \frac{KM}{r^2} + \frac{(rV_\varphi)^2}{r^3} \tag{A4}$$

Equation (A3) together with the relationship

$$r = r_o + \dot{r}_o t + O(t^2) \tag{A5}$$

put equation (A4) into the form

$$\ddot{r} = \ddot{r}_o - kt + O(t^2) \tag{A6}$$

wherein

$$k = \bar{\rho}\left(\frac{V_\varphi^3}{r}\right)_o\left(\frac{C_D A}{m}\right) + \left(\frac{\dot{r}_o}{r_o}\right)\left(3\ddot{r}_o + \frac{KM}{r_o^2}\right) \tag{A7}$$

Integration of equation (A6) yields

$$\left.\begin{aligned} \dot{r} &= \dot{r}_o + \ddot{r}_o t - \frac{kt^2}{2} + O(t^3) \\ r &= r_o + \dot{r}_o t + \ddot{r}_o \frac{t^2}{2} - \frac{kt^3}{6} + O(t^4) \end{aligned}\right\} \tag{A8}$$

To obtain the altitude time curve for a particular case, we first choose a value of $\bar{\rho}$ for the first step and evaluate k. The value of r versus t can then be established from equation (A8). The curve of r versus t also establishes a curve of ρ versus t for a given atmosphere. The time t_1 for which $\bar{\rho}$ satisfies the following relationship can easily be found

$$\bar{\rho} = \frac{1}{t_1}\int_o^{t_1} \rho \, dt \tag{A9}$$

Since $\bar{\rho}$ is the average value of ρ between $t = 0$ and $t = t_1$, the values of r_1, $\dot{r}_1$, and $\ddot{r}_1$ calculated from equations (A6) and (A7) for t_1 should be accurate. The values of r_1, $\dot{r}_1$, and $\ddot{r}_1$ are now used as initial values in the next step of the calculation. The next step is started by moving the zero of the time scale to t_1, choosing a new value of $\bar{\rho}$, and calculating a new value of k. Thus the process is continued step by step.

As a numerical example of this calculation consider a satellite launched in an equatorial orbit in an easterly direction with an initial altitude of 80 miles. The initial conditions necessary to proceed with the calculations are

$$\left.\begin{aligned} t_o &= 0 \text{ sec} \\ r_o &= a + h_o = 21{,}348{,}828 \text{ ft} \\ \dot{r}_o &= 0 \text{ ft/sec} \\ (V_\varphi)_o &= 25{,}678.862 \text{ ft/sec} \\ \frac{C_D A}{m} &= 1.0 \end{aligned}\right\} \qquad \text{(A10)}$$

At an altitude of 80 miles the density from reference 7 is $\rho = 2.96\times10^{-11}$ slugs per cubic foot. For the first step in the calculation of the trajectory let us choose a value of $\bar{\rho}$ slightly greater than the initial density, as follows,

$$\bar{\rho} = 3.019\times10^{-11} \text{ slugs/ft}^3 \qquad \text{(A11)}$$

and evaluate equation (A7) for k.

$$k = (3.019\times10^{-11}) \frac{(25{,}678.862)^3}{(21{,}348{,}828)} (1.0) + 0$$

$$= 2.3945\times10^{-5} \qquad \text{(A12)}$$

The considerations in selecting $\bar{\rho}$ are discussed subsequently.

With the value of k determined, equation (A8) is now used to establish a curve of r versus t. For t equal to 0, 400, 800, and 1200 seconds the respective values of r are found to be

$$t = 0 \text{ sec} \qquad r = 21{,}348{,}828 - \frac{2.3945\times10^{-5}(0)^3}{6}$$

$$= 21{,}348{,}828 \text{ ft}$$

$$t = 400 \text{ sec} \qquad r = 21{,}348{,}573 \text{ ft}$$

$$t = 800 \text{ sec} \qquad r = 21{,}346{,}785 \text{ ft}$$

$$t = 1200 \text{ sec} \qquad r = 21{,}341{,}932 \text{ ft}$$

These points also establish a curve of ρ versus t by the use of reference 9 to obtain ρ for a given altitude above the earth's surface. The corresponding values are

$$t = 0 \text{ sec} \qquad \rho = 2.96\times10^{-11} \text{ slugs/ft}^3$$

$$t = 400 \text{ sec} \qquad \rho = 2.98\times10^{-11} \text{ slugs/ft}^3$$

$$t = 800 \text{ sec} \qquad \rho = 3.18\times10^{-11} \text{ slugs/ft}^3$$

$$t = 1200 \text{ sec} \qquad \rho = 3.78\times10^{-11} \text{ slugs/ft}^3$$

From this curve of ρ versus t the value of t_1 which satisfies equation (A9) can be easily found, as is shown in the accompanying sketch, by making the two shaded areas under the curve equal. Performing this integration for this numerical example one finds that

$$t_1 = 821 \text{ sec} \qquad \text{(A13)}$$

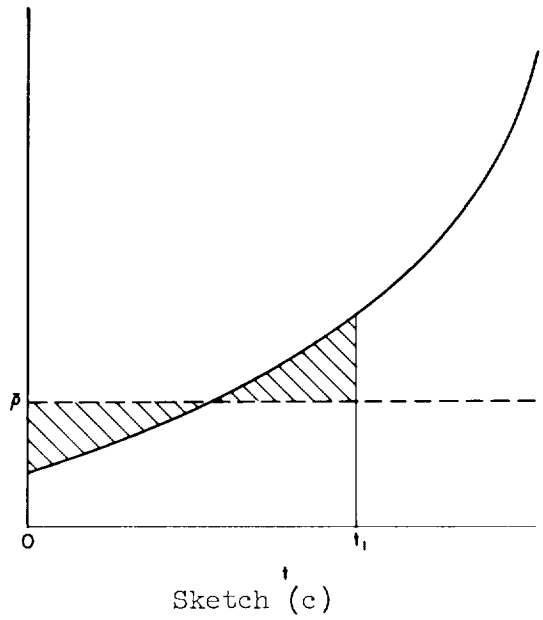

Sketch (c)

Now, using the values from equations (A10), (A12), and (A13) and inserting them in equations (A6) and (A8) yields the quantities

$$r_1 = 21{,}348{,}828 - \frac{(2.3945\times10^{-5})(821)^3}{6.0}$$

$$= 21{,}346{,}619 \text{ ft}$$

$$\dot{r}_1 = -\frac{(2.3945\times10^{-5})(821)^2}{2.0}$$

$$= -8.06996 \text{ ft/sec}$$

$$\ddot{r}_1 = -(2.3945\times10^{-5})(821)$$

$$= -0.01966 \text{ ft/sec}^2$$

Therefore, at $t_1 = 821$ seconds the quantities specifying the satellite's position and motion are

$$\left.\begin{aligned} r_1 &= 21{,}346{,}619 \text{ ft} \\ \dot{r}_1 &= -8.06996 \text{ ft/sec} \\ \ddot{r}_1 &= -0.01966 \text{ ft/sec}^2 \\ (V_\varphi)_1 &= 25{,}678.862 \text{ ft/sec} \end{aligned}\right\} \tag{A14}$$

These values are now used as initial values in the next step of the calculation. The zero of the time scale is shifted to correspond to t_1, and a new value of $\bar{\rho}$ must be chosen. The value of r_1 corresponds to an altitude above the earth's surface of 420,191 feet for which the density (ref. 7) is 3.205×10^{-11} slugs per cubic foot. As the average density for the next step, let us, therefore, choose a new value of

$$\bar{\rho} = 4.30\times10^{-11} \text{ slugs/ft}^3 \tag{A15}$$

With this value and equations (A14) the calculation of k (eq. (A7)) is repeated and is found to be

$$k = 2.2452\times10^{-5}$$

Now the curve of r versus t is determined from equation (A8) and the corresponding densities are determined from reference 9. These are

t, sec	r, ft	ρ, slugs/ft^3
0	21,346,619	3.205×10^{-11}
400	21,341,579	3.830×10^{-11}
800	21,331,956	5.390×10^{-11}
1200	21,316,314	9.650×10^{-11}

Integrating graphically as before

$$t_2 - t_1 = 959 \text{ sec} \tag{A16}$$

and equations (A6) and (A8) thus give

$$\left.\begin{aligned} r_2 &= 21{,}326{,}540 \text{ ft} \\ \dot{r}_2 &= -37.24824 \text{ ft/sec} \\ \ddot{r}_2 &= -0.04119 \text{ ft/sec}^2 \end{aligned}\right\} \tag{A17}$$

Therefore, at $t_2 = 1780$ seconds, these quantities plus V_φ, obtained from equation (A3) specify the satellite's position and motion.

These quantities thus become the initial conditions for the next step and the calculation is repeated.

Let us now consider the factors entering the choice of $\bar{\rho}$. For entry from circular orbits, as in the present example, the value of $\bar{\rho}$ should be 1 or 2 percent greater than the initial density, ρ_o. In the calculation of figure 11 for the long time interval, it was decided a priori to go to 3000 seconds in about four steps. The values of $\bar{\rho}/\rho_o$ for each step are shown in the following table:

Time interval	$\bar{\rho}/\rho_o$	ρ_1/ρ_o
0 - 821 sec	1.020	1.083
821 - 1780 sec	1.342	2.031
1780 - 2425 sec	1.966	3.932
2425 - 2875 sec	3.125	9.415

Because the density changes slowly with altitude at first, a large initial value of $\bar{\rho}/\rho_o$ would give a very large time interval. This is to be avoided since the present method is based on power series in time. Once the curve of ρ versus t is established in the first interval, the values of $\bar{\rho}/\rho_o$ for subsequent intervals to obtain given intervals in time can be estimated by extrapolating the curve.

To study the effects of time interval, the calculation was also made in about eight steps instead of four. As expected, the calculation with more steps remains closer to the machine solution at large values of the time. In any particular case, it is best to do the calculation with two different time intervals to be sure of the range of accuracy of the calculations.

It might be mentioned, in conclusion, that the present method can be applied to an atmosphere of arbitrary density-altitude relationship.

APPENDIX B

APPROXIMATE EXPRESSION FOR ECCENTRICITY FOR VALUE OF V_φ SMALL COMPARED TO V_c

It is possible on the basis of energy considerations to obtain a simple expression for the eccentricity for values of V_φ/V_c small compared to unity. The starting point is equation (41) which relates the eccentricity to certain quantities as follows

$$1 - E^2 = \frac{L_o}{pl} \tag{B1}$$

From the definitions of L_o and p we find

$$\frac{L_o}{pl} = \frac{\xi_o^2}{KM}\left(\frac{\xi^2}{\xi_o^2}\right)\left(\frac{1}{l}\right) = \frac{\xi^2}{KMl} \tag{B2}$$

The length of the semimajor axis l is related to the total energy for a circular force field. The kinetic energy for unit mass is $V^2/2$ and the potential energy per unit mass is $-KM/r$. Thus the total energy E is

$$E = \frac{V^2}{2} - \frac{KM}{r} = \frac{V^2}{2} - V_c^2 \tag{B3}$$

Since the total energy depends only on the length of the major axis independent of the eccentricity, we have (ref. 3)

$$E = -\frac{KM}{2l} = \frac{V^2}{2} - V_c^2 \tag{B4}$$

The expression for L_o/pl thus becomes

$$\begin{aligned}\frac{L_o}{pl} &= -\left(\frac{V_\varphi^2 r^2}{KM}\right)\left(\frac{2}{KM}\right)\left(\frac{V^2}{2} - V_c^2\right) \\ &= -2\left(\frac{V_\varphi^2}{V_c^2}\right)\left(\frac{V^2}{2V_c^2} - 1\right)\end{aligned} \tag{B5}$$

Thus from equation (B1)

$$1 - E^2 = (1 - E)(1 + E) = 2\left(1 - \frac{V^2}{2V_c^2}\right)\left(\frac{V_\varphi}{V_c}\right)^2 \tag{B6}$$

For E near unity

$$E \approx 1 - \left(1 - \frac{V^2}{2V_c^2}\right)\left(\frac{V_\varphi}{V_c}\right)^2 \tag{B7}$$

It is clear that E approaches unity as the path becomes vertical.

At the other limit assume that V_φ is nearly equal to V_c so that

$$\frac{V_\varphi}{V_c} = 1 + \epsilon \tag{B8}$$

where ϵ is a small quantity. Let us rewrite equation (B7) in the form

$$E^2 = \left(\frac{V_\varphi^2}{V_c^2} - 1\right)^2 + \left(\frac{\dot{r}}{V_\varphi}\right)^2\left(\frac{V_\varphi}{V_c}\right)^4 \tag{B9}$$

or

$$E^2 = \left[2\epsilon\left(1 + \frac{\epsilon}{2}\right)\right]^2 + \left(\frac{\dot{r}}{V_\varphi}\right)^2(1 + 2\epsilon + \epsilon^2)^2 \tag{B10}$$

For $V_\varphi = V_c$ or very close to it, we thus have

$$E^2 \approx \left|\frac{\dot{r}}{V_\varphi}\right|^2 + 4\epsilon^2$$

APPENDIX C

CHANGE IN PERIGEE ALTITUDE DUE TO OBLATENESS

GRAVITATIONAL FIELD FOR EQUATORIAL ORBITS

The specific question considered here concerns a satellite in a circular orbit without oblateness forces at time $t = 0$: When the oblateness gravitational field is suddenly "turned on," what happens to the perigee radius, r_p? Let r_a be the radius of the circular orbit without oblateness forces, which becomes the apogee radius as soon as oblateness forces are turned on. From the previous appendix it is known that the total energy is related to the length $2l$ of the major axis (without oblateness) by equation (B4).

$$E = - \frac{KM}{2l} \tag{C1}$$

A change in energy ΔE is such that

$$\frac{\Delta E}{E} = - \frac{\Delta l}{l} \tag{C2}$$

Now for an equatorial orbit the energy balance with $V_\varphi = V_c$ and with no oblateness is such that the orbit is circular. With oblateness the energy balance requires that $V_\varphi = V_{co}$ for a circular orbit. Thus if $V_\varphi = V_c$ with oblateness, there is a kinetic energy deficiency of $(V_{co}^2 - V_c^2)/2$ per unit mass for a circular orbit. This energy deficiency causes a change in length of the major axis $\Delta 2l$ of $r_a - r_p$ since the orbit has the same apogee radius with or without oblateness. Thus

$$r_a - r_p = - \frac{2l\Delta E}{E} = - \frac{l}{E} V_{co}^2 \left(1 - \frac{V_c^2}{V_{co}^2} \right) \tag{C3}$$

with

$$\left. \begin{aligned} E &\approx - \frac{V_c^2}{2} \\ \frac{V_c^2}{V_{co}^2} &\approx 1 - \frac{6\mu a^2}{r^2} \end{aligned} \right\} \tag{C4}$$

equation (C3) becomes

$$(r_a - r_p) \approx 12\mu \left(\frac{a^2}{r^2} \right) r_a \tag{C5}$$

REFERENCES

1. Taratynova, G. P.: The Motion of an Artificial Satellite in the Noncentral Gravitational Field of the Earth in the Presence of Atmospheric Resistance. U. S. Joint Pub. Res. Serv. Rep. 187: Symposium of Soviet Research on Artificial Earth Satellites and Related Subjects, pt. 1, 25 Jan. 1958, pp. 69-81. (Trans. of USPEKHI FIZICHESKIKH NAUK, Progress in Physical Sciences, vol. 63, no. 1a, Sept. 1957, pp. 51-58)

2. Blitzer, Leon, Weisfeld, Morris, and Wheelon, Albert D.: Perturbations of a Satellite's Orbit Due to the Earth's Oblateness. Jour. Appl. Phys., vol. 27, no. 10, Oct. 1956, pp. 1141-1149.

3. Henry, Irvin G.: Lifetimes of Artificial Satellites of the Earth. Jet Propulsion, vol. 27, no. 1, Jan. 1957, pp. 21-24, 27.

4. Chapman, Dean R.: An Approximate Analytical Method for Studying Re-entry Into Planetary Atmospheres. NACA TN 4276, 1958.

5. Allen, H. J., and Eggers, A. J., Jr.: A Study of the Motion and Aerodynamic Heating of Missiles Entering the Earth's Atmosphere at High Supersonic Speeds. NACA TN 4047, 1957.

6. Gazley, Carl, Jr.: Deceleration and Heating of a Body Entering a Planetary Atmosphere From Space. Rand Rep. P-955, Feb. 1957.

7. Houston, William V.: Principles of Mathematical Physics. Second ed., McGraw-Hill Book Co., Inc., 1948.

8. Fowle, Frederick E.: Smithsonian Physical Tables. Eighth ed. (rev.), Smithsonian Inst., Washington D. C., 1934, Table 716, p. 570.

9. Minzner, R. A., and Ripley, W. S.: The ARDC Model Atmosphere. AF Survey in Geophysics, no. 86, AF Cambridge Res. Center, TN 56-204, Dec. 1956.

10. Harris, I., and Jastrow, R.: Upper Atmosphere Densities From Minitrack Observations on Sputnik I. Science, vol. 127, no. 3296, 28 Feb. 1958, pp. 471-472.

11. Flügge, S.: Handbuch der Physik, Band XLVII, Geophysik I, Springer-Verlag, 1956, p. 636.

12. Charters, A. C.: The Linearized Equations of Motion Underlying the Dynamic Stability of Aircraft, Spinning Projectiles, and Symmetrical Missiles. NACA TN 3350, 1955, p. 39.

13. Roberson, Robert E.: Orbital Behaviors of Earth Satellites. Jour. Franklin Inst., vol. 264, no. 4, Oct. 1957, pp. 269-285.

14. Linnell, R. D.: Vertical Re-entry Into the Earth's Atmosphere for Both Light and Heavy Bodies. Jet Propulsion, vol. 28, no. 5, May 1958, pp. 329-330.

15. King-Hele, D. G., and Gilmore, D. M. C.: The Effect of the Earth's Oblateness on the Orbit of a Near Satellite. R.A.E. TN G.W. 475, Oct. 1957.

TABLE I.- PERCENTAGE EFFECT OF OBLATENESS GRAVITATIONAL FIELD ON RANGE

$C_DA/m = 1$				
$\dot{r}_o/(V_\varphi)_o$	0	-0.01	-0.05	-0.10
ψ_4, miles	-4406.562	3582.562	948.577	526.382
λ_4, miles	20,060.089	2614.743	545.045	335.566
s_4, miles	19,279.667	4201.140	1089.919	624.226
t, sec	4355	1199	538	426
$(\psi_2 - \psi_1)/s_4$	-.330	-.042	-.003	-.001
$(\lambda_2 - \lambda_1)/s_4$	-.365	-.067	-.001	.000
$(\psi_4 - \psi_3)/s_4$	-.366	-.042	-.003	-.003
$(\lambda_4 - \lambda_3)/s_4$	-.334	-.070	-.001	-.005
$C_DA/m = 10$				
ψ_4, miles	3344.785	2527.760	751.924	427.021
λ_4, miles	10,539.586	1689.927	640.422	480.512
s_4, miles	8975.380	2974.090	984.494	642.061
t, sec	2801	1594	1158	1068
$(\psi_2 - \psi_1)/s_4$	.090	-.023	-.002	-.001
$(\lambda_2 - \lambda_1)/s_4$	-.095	-.018	-.001	.000
$(\psi_4 - \psi_3)/s_4$	.094	-.024	-.002	-.001
$(\lambda_4 - \lambda_3)/s_4$	-.091	-.019	-.001	.000

TABLE II.- PERCENTAGE EFFECT OF ATMOSPHERIC ROTATION ON RANGE

$C_DA/m = 1$				
$\dot{r}_o/(V\varphi)_o$	0	-0.01	-0.05	-0.10
ψ_4, miles	-4406.562	3582.562	948.577	526.382
λ_4, miles	20,060.089	2614.743	545.045	335.566
s_4, miles	19,279.667	4201.140	1089.919	624.226
t, sec	4355	1199	538	426
$(\psi_3 - \psi_1)/s_4$	.040	.006	.003	.004
$(\lambda_3 - \lambda_1)/s_4$	.033	.034	.087	.148
$(\psi_4 - \psi_2)/s_4$	.004	.005	.003	.002
$(\lambda_4 - \lambda_2)/s_4$	.064	.032	.087	.143
$C_DA/m = 10$				
ψ_4, miles	3344.785	2527.760	751.924	427.021
λ_4, miles	10,539.586	1689.927	640.422	480.512
s_4, miles	8975.380	2974.090	984.494	642.061
t, sec	2801	1594	1158	1068
$(\psi_3 - \psi_1)/s_4$	-.017	.007	.003	.002
$(\lambda_3 - \lambda_1)/s_4$	.045	.103	.291	.438
$(\psi_4 - \psi_2)/s_4$	-.013	.006	.003	.002
$(\lambda_4 - \lambda_2)/s_4$	.049	.103	.291	.438

TABLE III.- CALCULATED QUANTITIES FOR EQUATORIAL ORBIT

t, sec	h, ft	V_φ, ft/sec	$-\dot{r}$, ft/sec	λ, radians	V_c, ft/sec	V_φ/V_c
0	422,400	25,678.860	0	0	25,678.86	1.000000
606	421,753	25,674.298	3.899	.7288	25,679.25	.999807
1669	407,830	25,677.980	24.045	2.0076	25,687.62	.999624
1955	400,009	25,682.181	30.820	2.3519	25,692.33	.999605
2442	381,881	25,689.336	44.438	2.9387	25,703.27	.999458
2588	375,008	25,690.380	49.840	3.1147	25,707.41	.999338
2916	355,947	25,685.460	68.485	3.5104	25,718.92	.998699
2998	350,039	25,680.795	75.852	3.6094	25,722.50	.998378
3200	332,175	25,651.831	104.165	3.8532	25,740.28	.996834
3400	306,036	25,543.869	167.173	4.0943	25,749.14	.991989
3500	286,112	25,315.656	239.939	4.2142	25,761.21	.982704
3665	220,154	22,022.188	696.182	4.4043	25,801.36	.853528
3696	195,186	19,039.298	923.976	4.4346	25,816.60	.737483
3721	169,602	15,017.882	1,116.853	4.4550	25,832.27	.581361
3746	140,388	9,474.258	1,183.196	4.4696	25,850.16	.366507
3755	129,886	7,368.195	1,144.695	4.4732	25,856.61	.284964
3764	119,859	5,464.839	1,079.841	4.4759	25,862.77	.211301
3773	110,478	3,896.195	1,003.839	4.4779	25,868.54	.150615
3784	99,935	2,479.298	915.170	4.4796	24,875.03	.095818
3795	90,295	1,529.855	840.117	4.4806	25,880.96	.059111
3805	82,195	960.579	781.004	4.4812	25,885.94	.037108
3821	70,436	422.641	688.208	4.4817	25,893.28	.016315
3837	60,268	159.390	580.798	4.4819	25,899.46	.006154
3857	49,986	35.608	452.853	4.4820	25,905.81	.001374
3882	40,103	3.564	347.173	4.4820	25,911.91	.000138
3915	30,011	.088	274.510	4.4820	25,918.16	.000003
3934	25,041	.008	249.848	4.4820	25,921.23	0
3955	20,023	0	228.336	4.4820	25,924.33	0
3978	14,998	0	209.522	4.4820	25,927.44	0
4003	9,973	0	192.983	4.4820	25,930.56	0
4030	4,965	0	178.392	4.4820	25,933.65	0
4058	151	0	165.883	4.4820	25,936.64	0

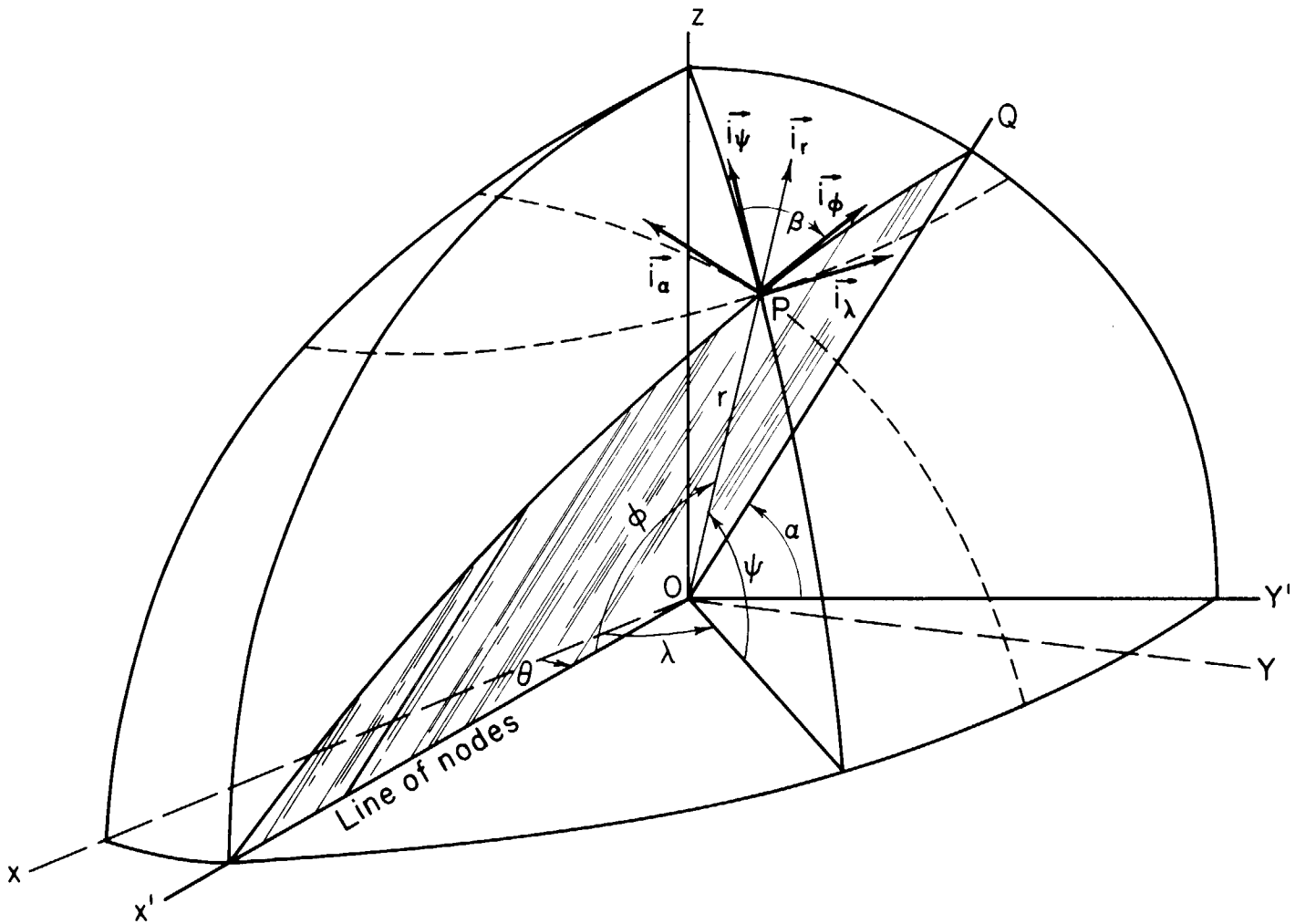

(a) Trajectory coordinates.

Figure 1.- Coordinate systems and notation.

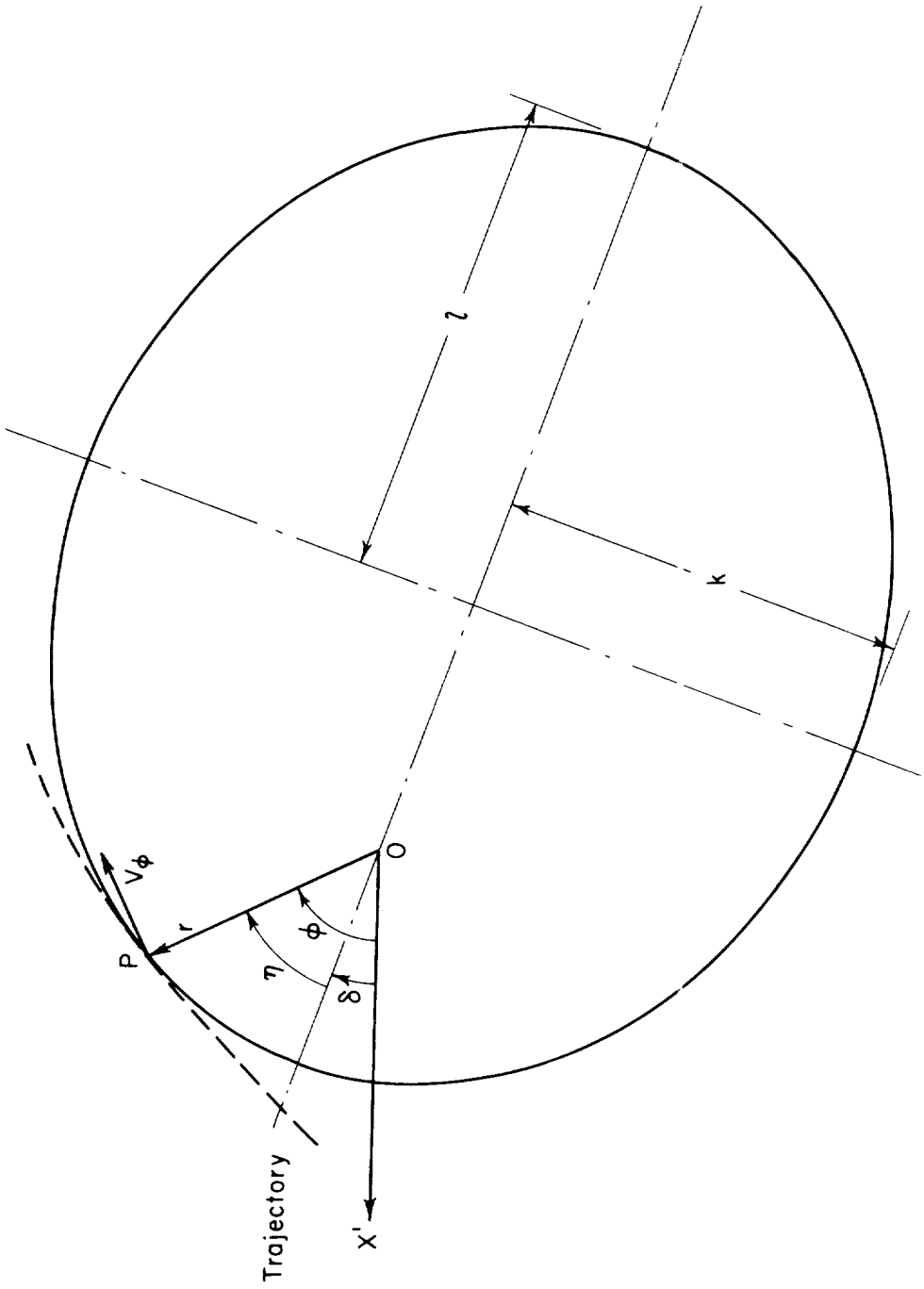

(b) Instantaneous ellipse coordinates.

Figure 1.- Concluded.

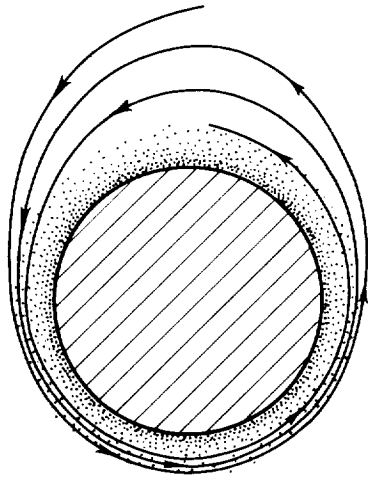

(a) Circularization of ellipse

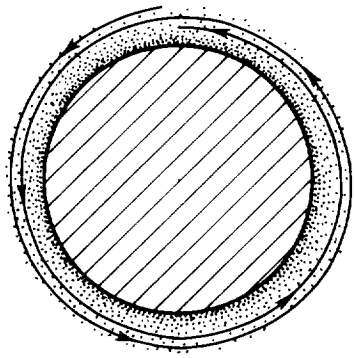

(b) Spiral decay

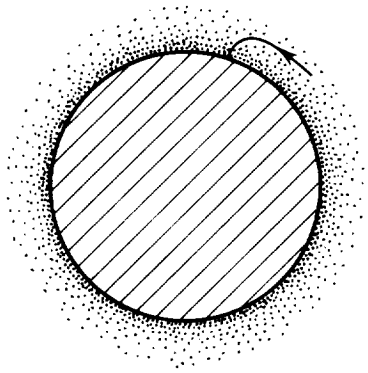

(c) Terminal phase

Figure 2.- Phases in trajectory of satellite.

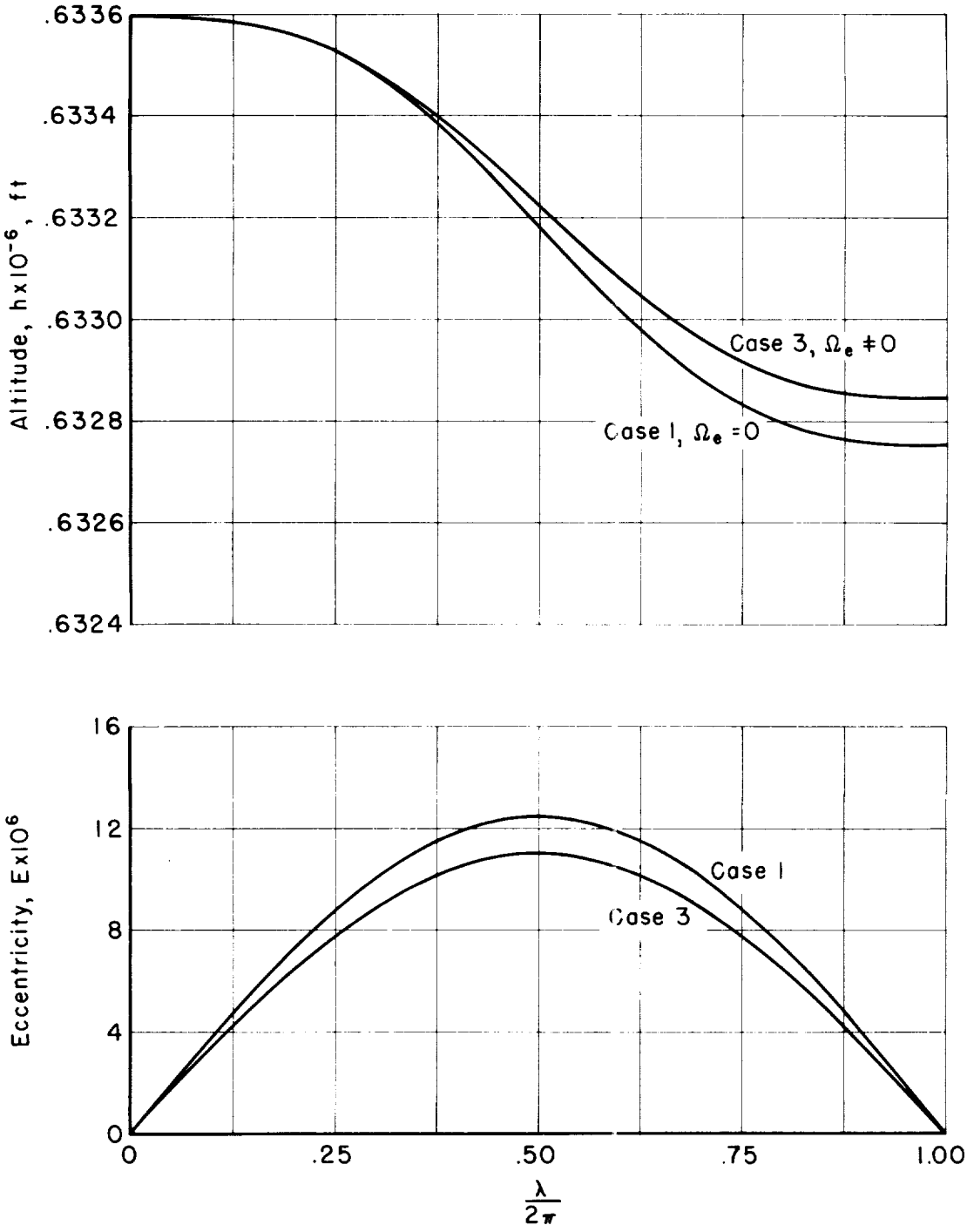

(a) $C_D A/m = 1$; cases 1 and 3; $\mu = 0$.

Figure 3.- Periodic variations of altitude and eccentricity for equatorial orbits; h_o = 120 statute miles.

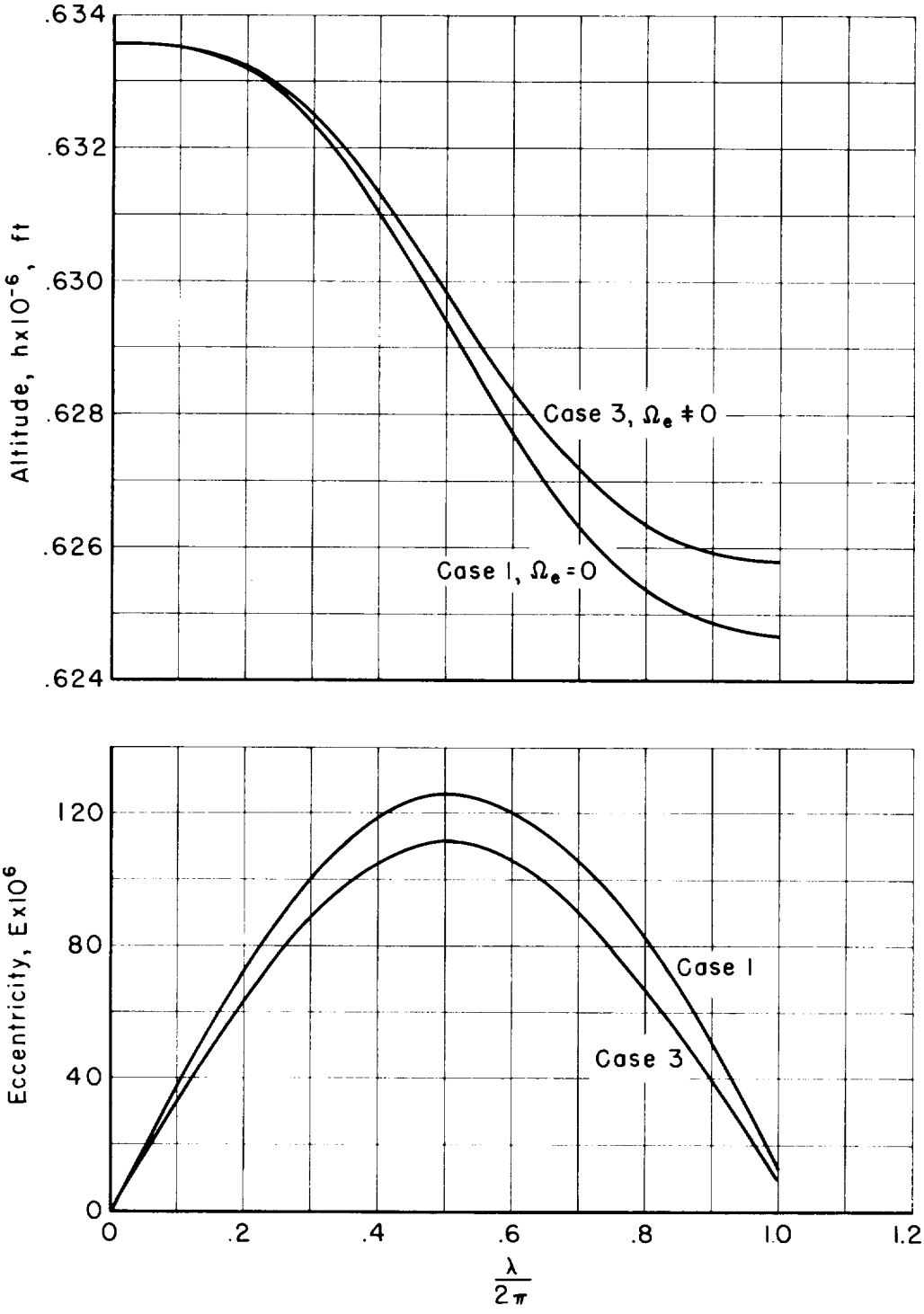

(b) $C_D A/m = 10$; cases 1 and 3; $\mu = 0$.

Figure 3.- Continued.

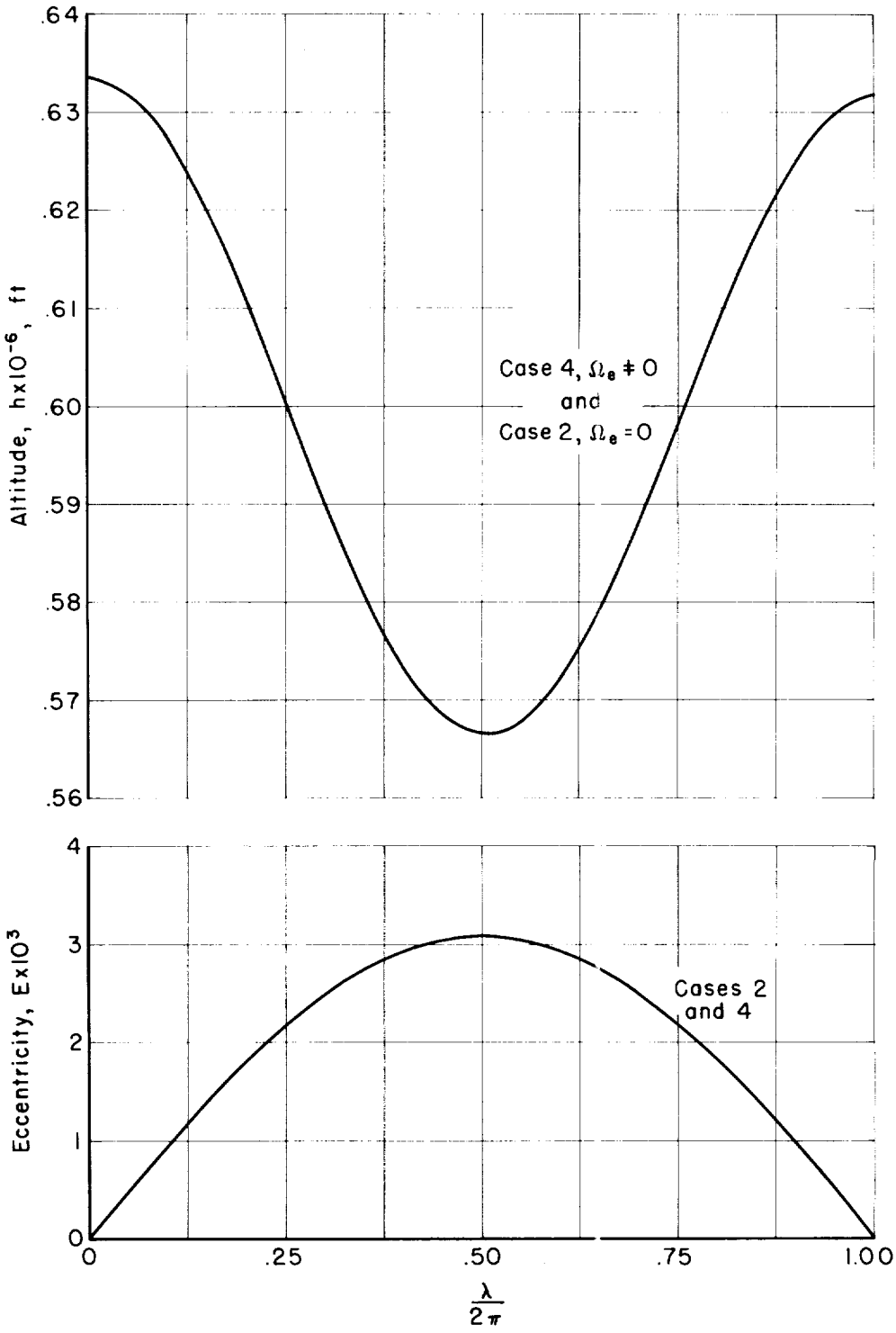

(c) $C_D A/m = 1$; cases 2 and 4; $\mu \neq 0$.

Figure 3.- Continued.

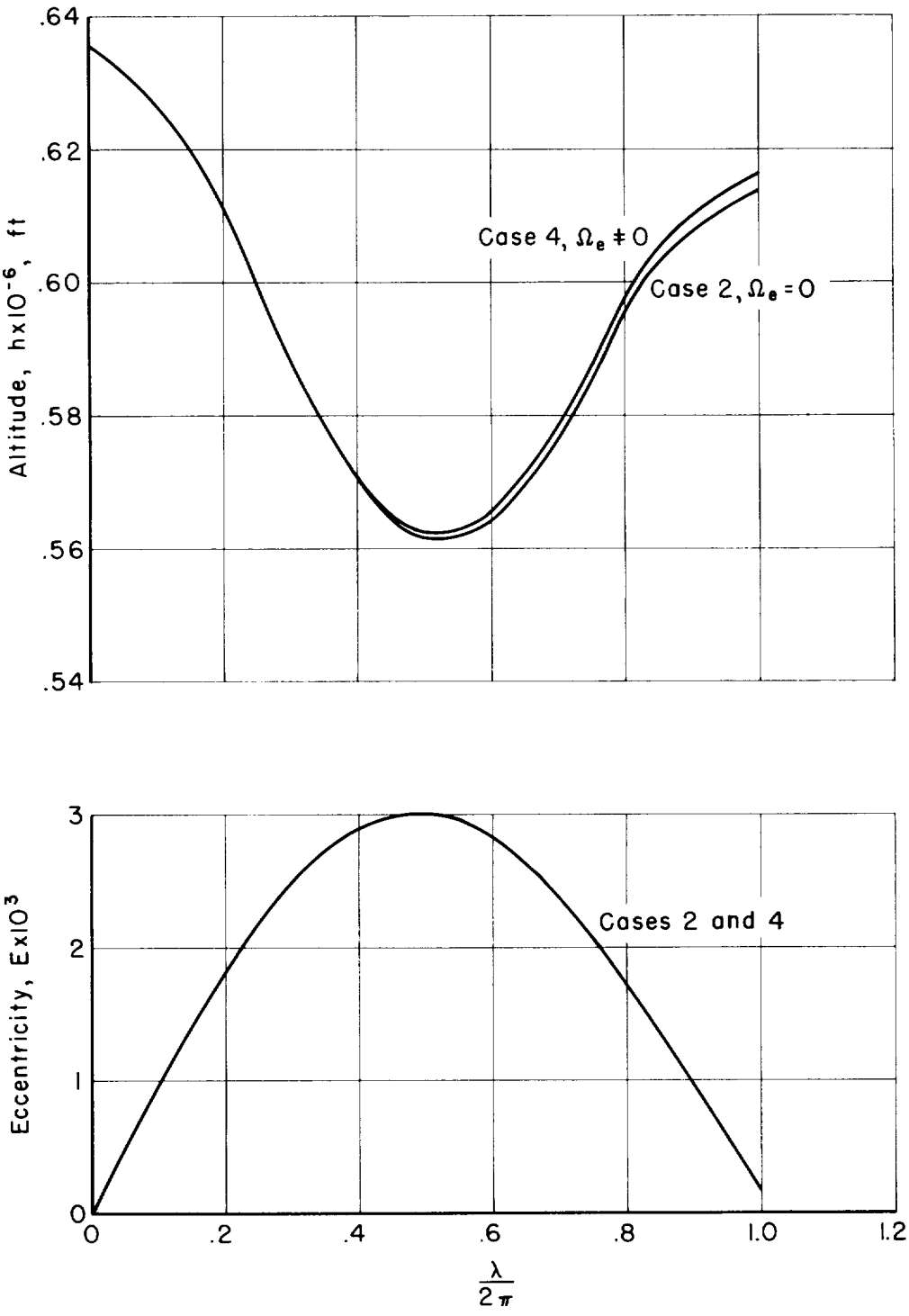

(d) $C_DA/m = 10$; cases 2 and 4; $\mu \neq 0$.

Figure 3.- Concluded.

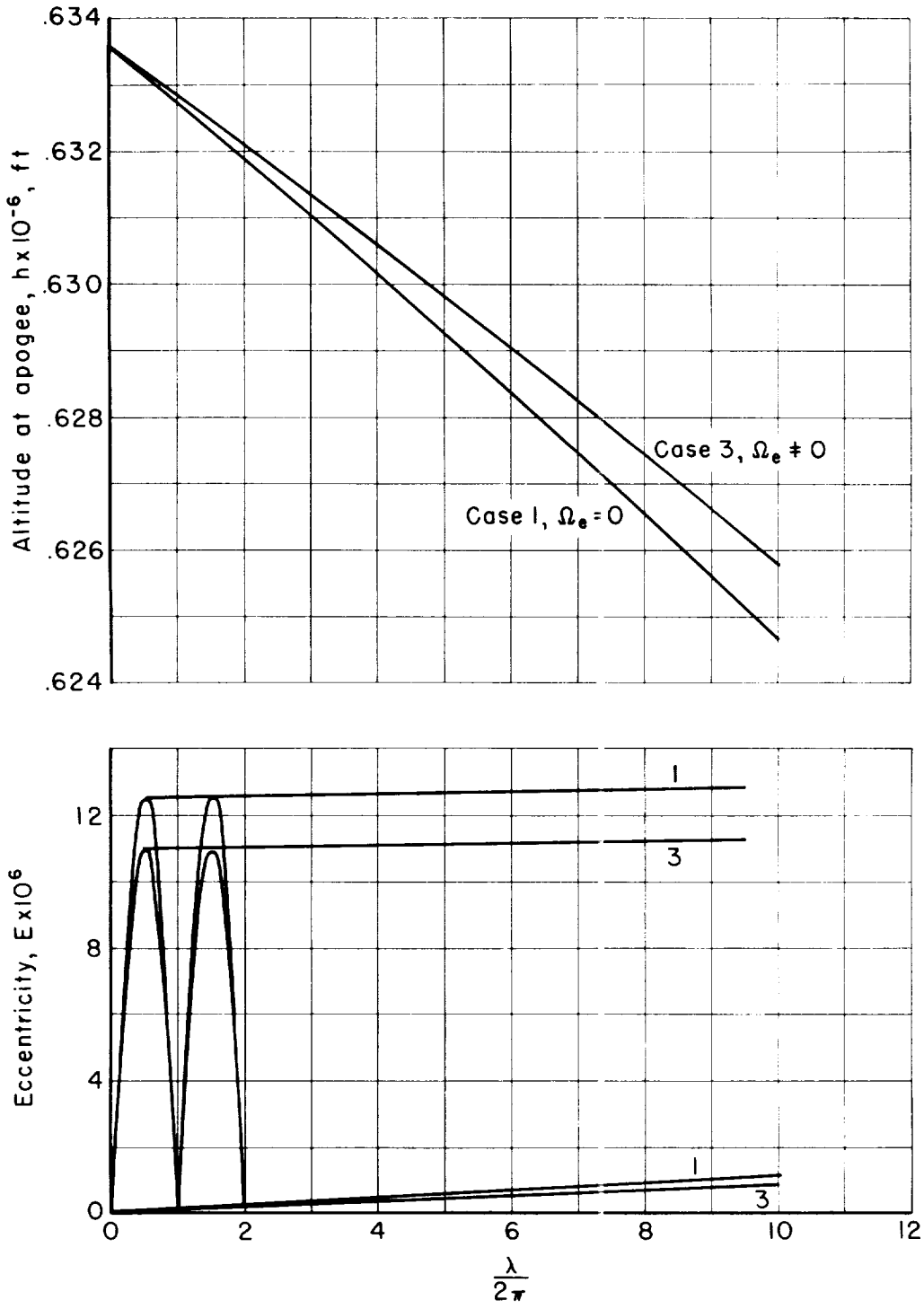

(a) $C_DA/m = 1$; cases 1 and 3; $\mu = 0$.

Figure 4.- Secular trends in altitude and eccentricity for equatorial orbits; h_o = 120 statute miles.

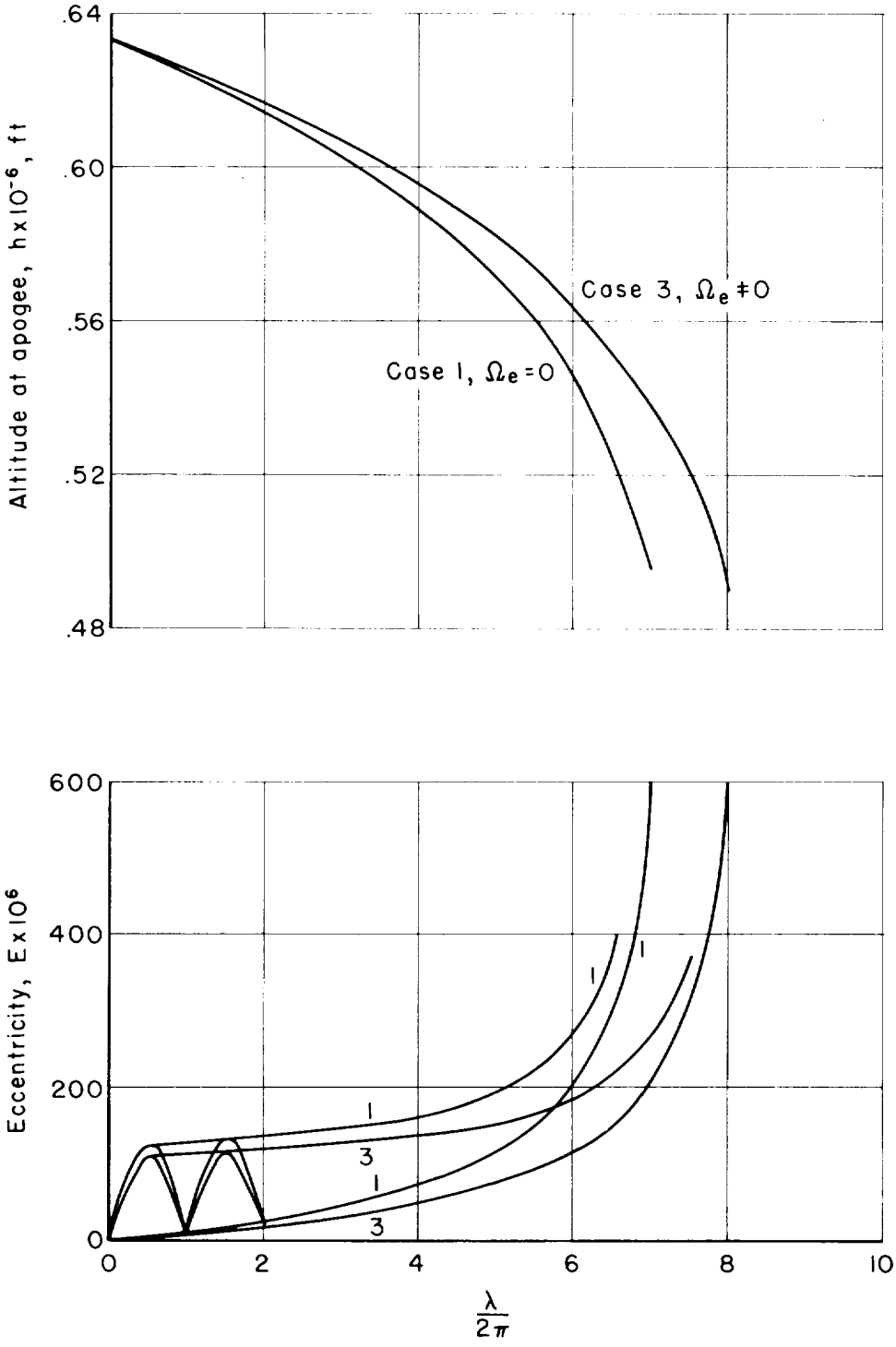

(b) $C_D A/m = 10$; cases 1 and 3; $\mu = 0$.

Figure 4.- Continued.

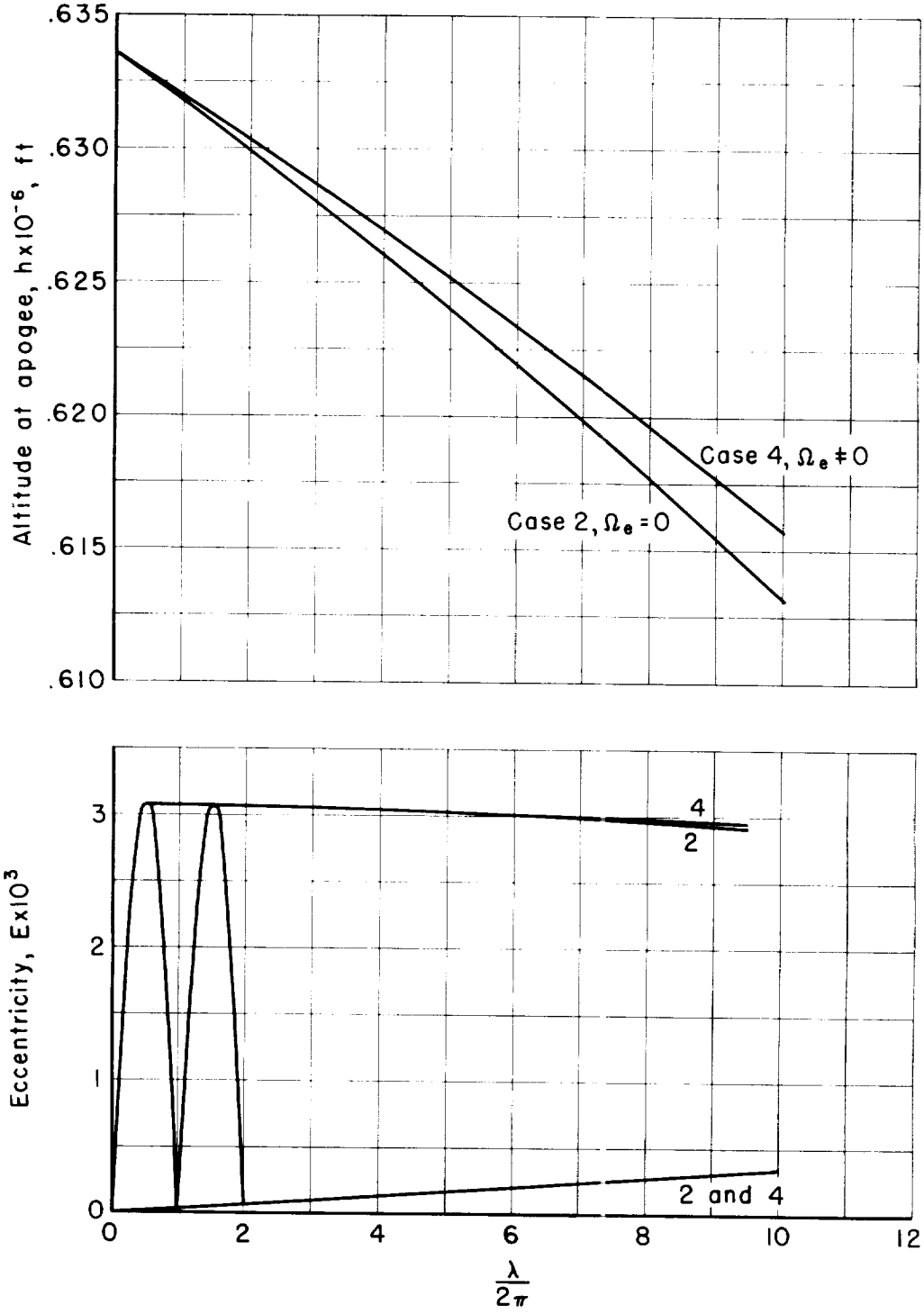

(c) $C_D A/m = 1$; cases 2 and 4; $\mu \neq 0$.

Figure 4.- Continued.

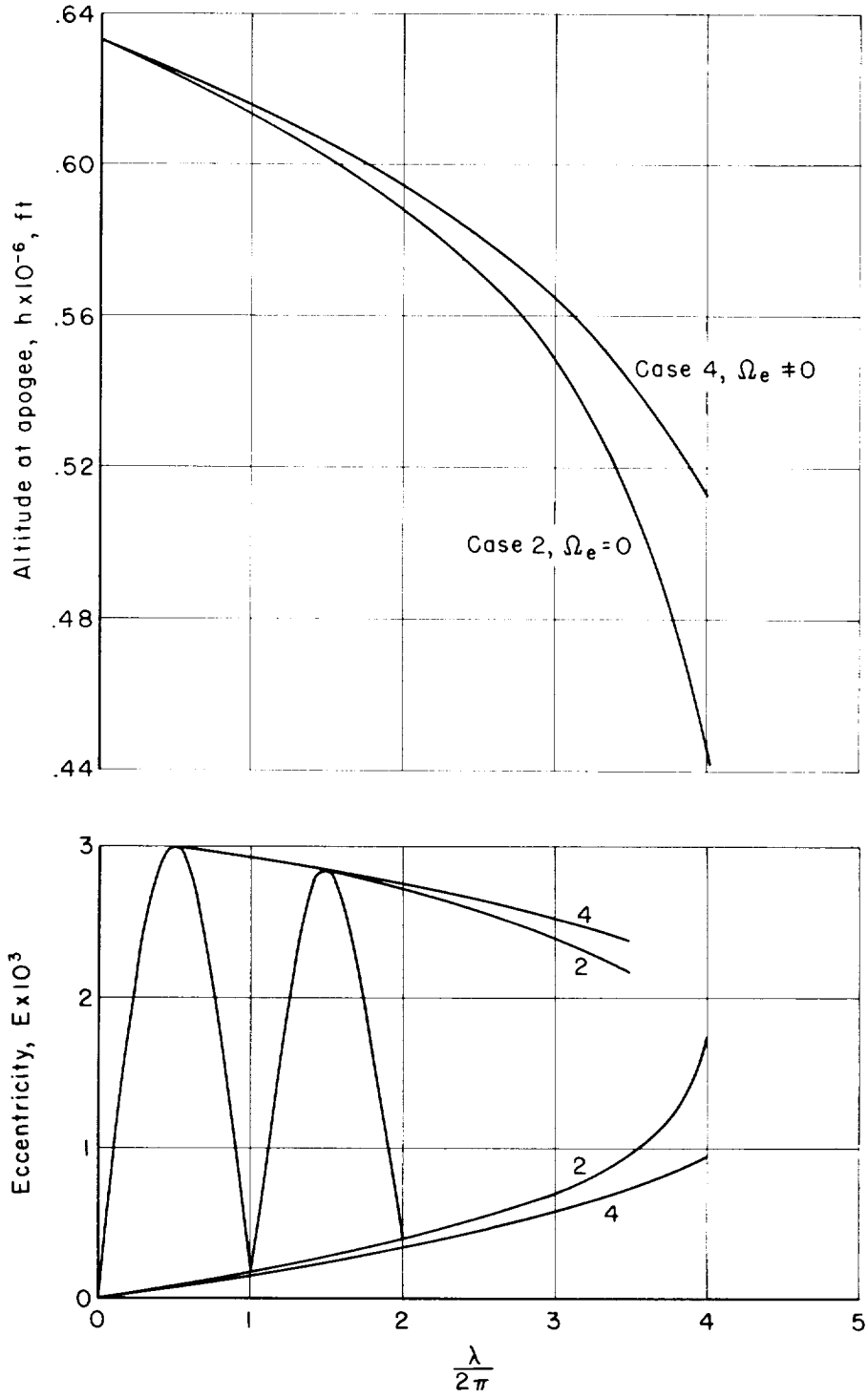

(d) $C_DA/m = 10$; cases 2 and 4; $\mu \neq 0$.

Figure 4.- Concluded.

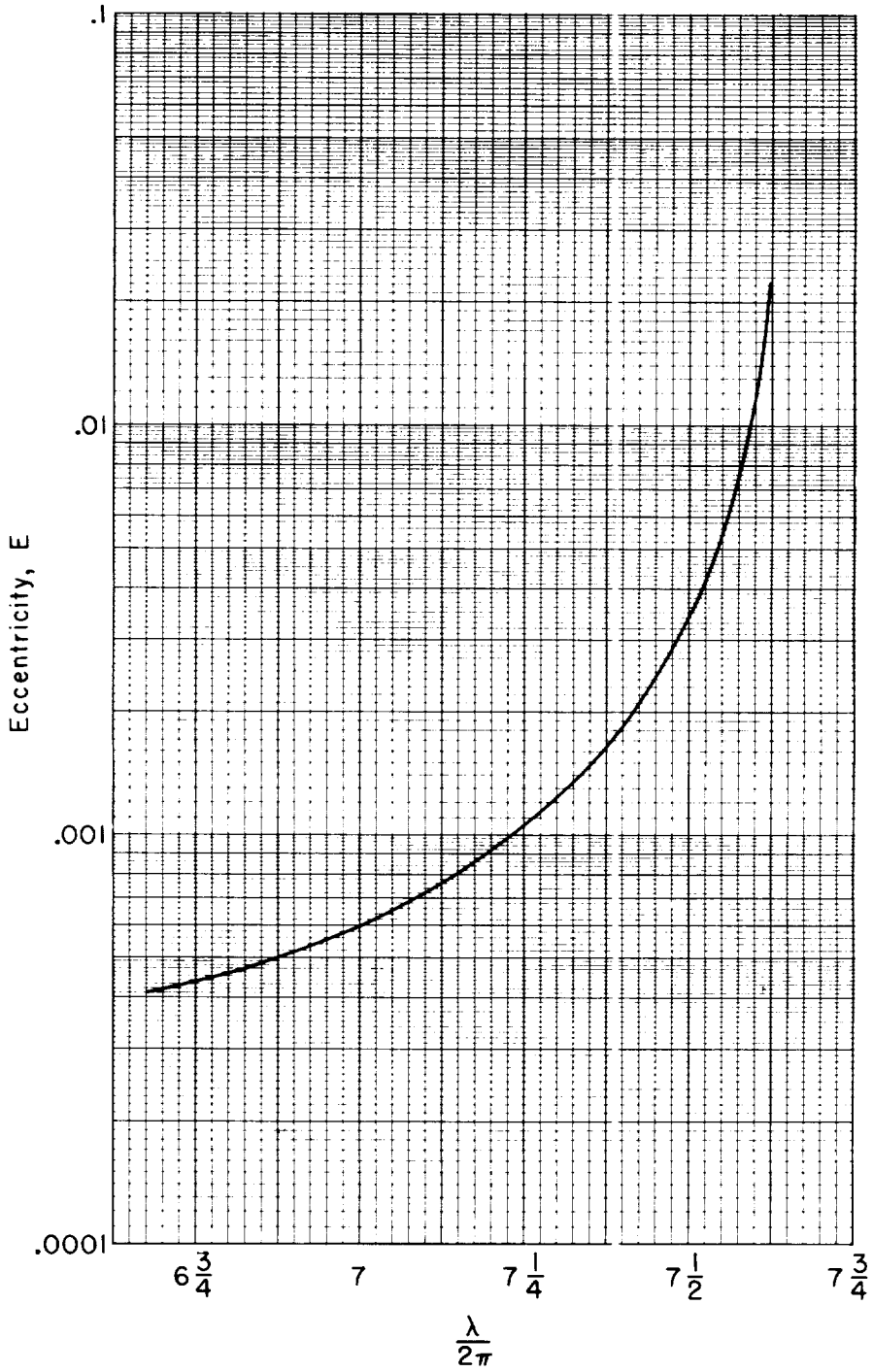

(a) $C_DA/m = 10$; case 1; $\Omega_e = 0$, $\mu = 0$.

Figure 5.- Eccentricity variation for equatorial orbits; h_o = 120 statute miles.

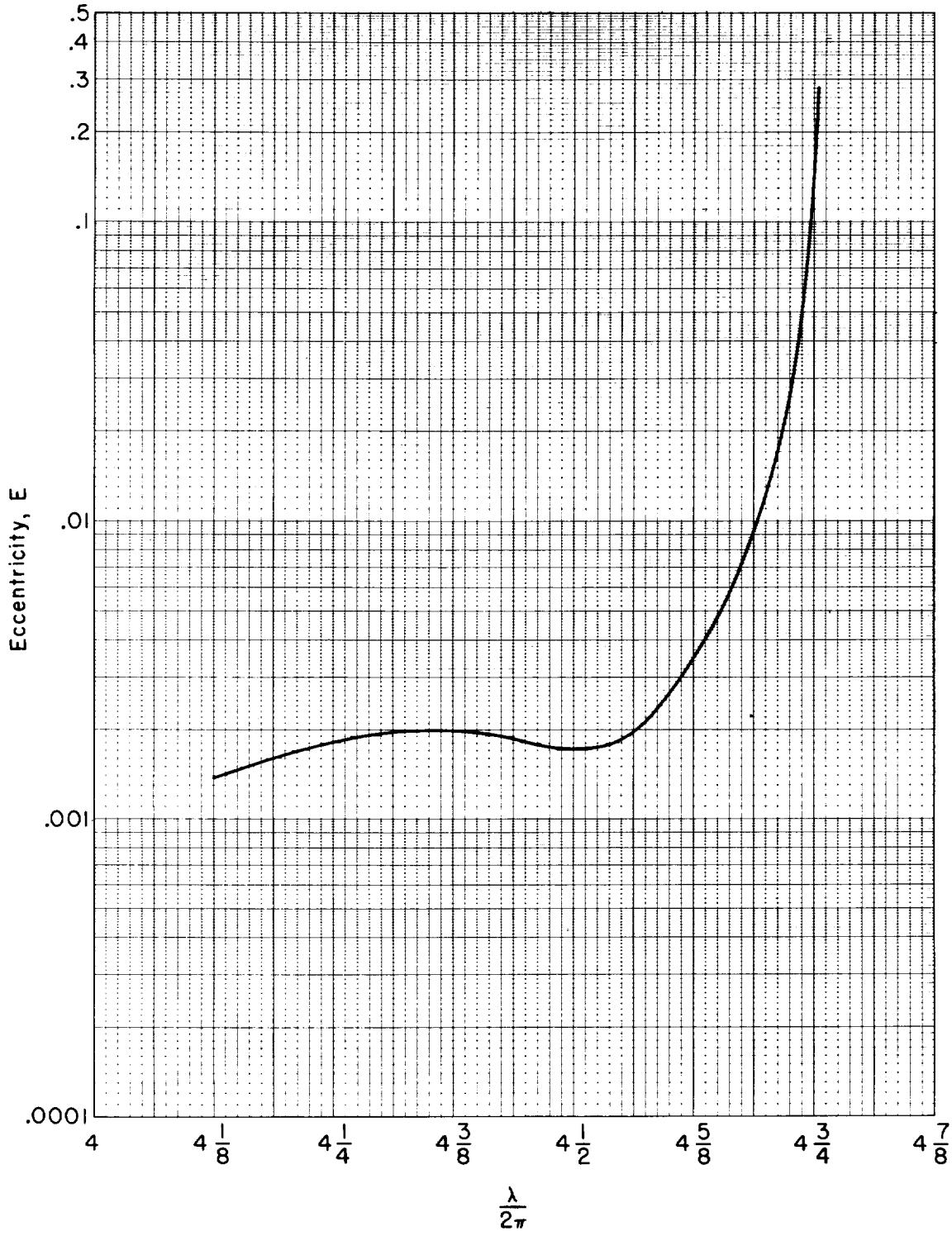

(b) $C_DA/m = 10$; case 4; $\Omega_e \neq 0$, $\mu \neq 0$.

Figure 5.- Concluded.

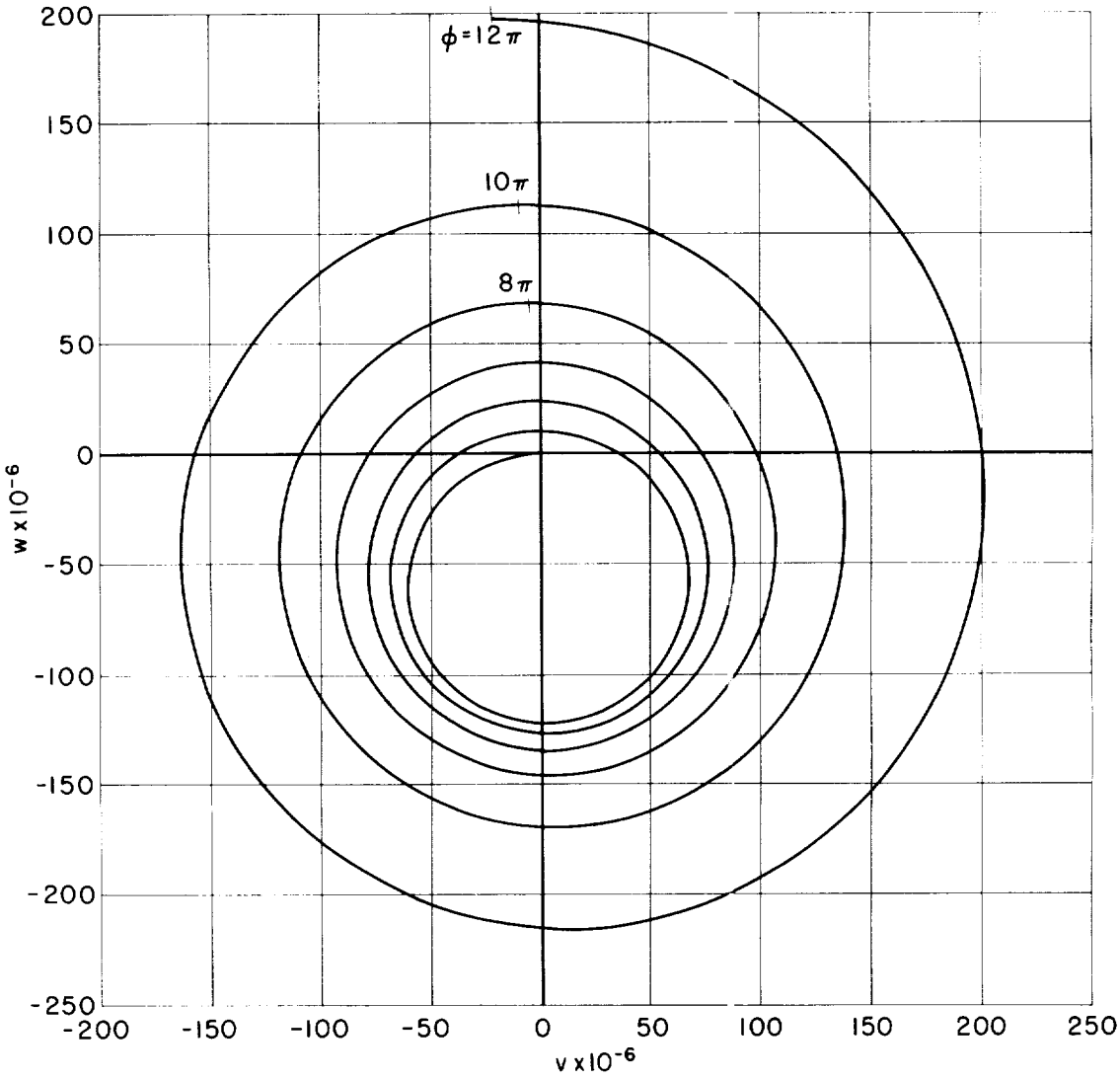

(a) Position of line of apsides, δ, as polar angle.

Figure 6.- Position of line of apsides; $C_DA/m = 10$, $h_o = 120$ statute miles, case 1; $\Omega_e = 0$, $\mu = 0$.

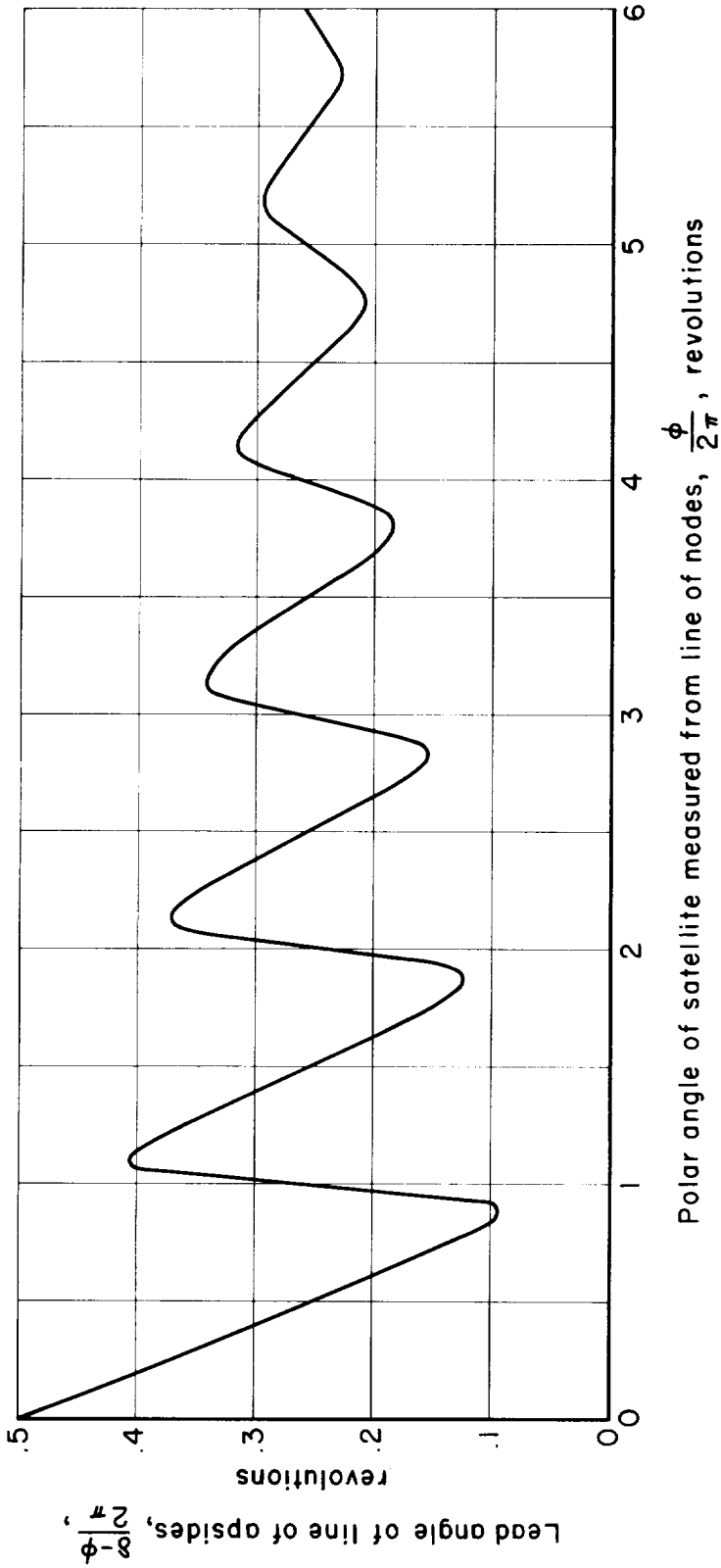

(b) Position of line of apsides, δ, measured from satellite.

Figure 6.- Concluded.

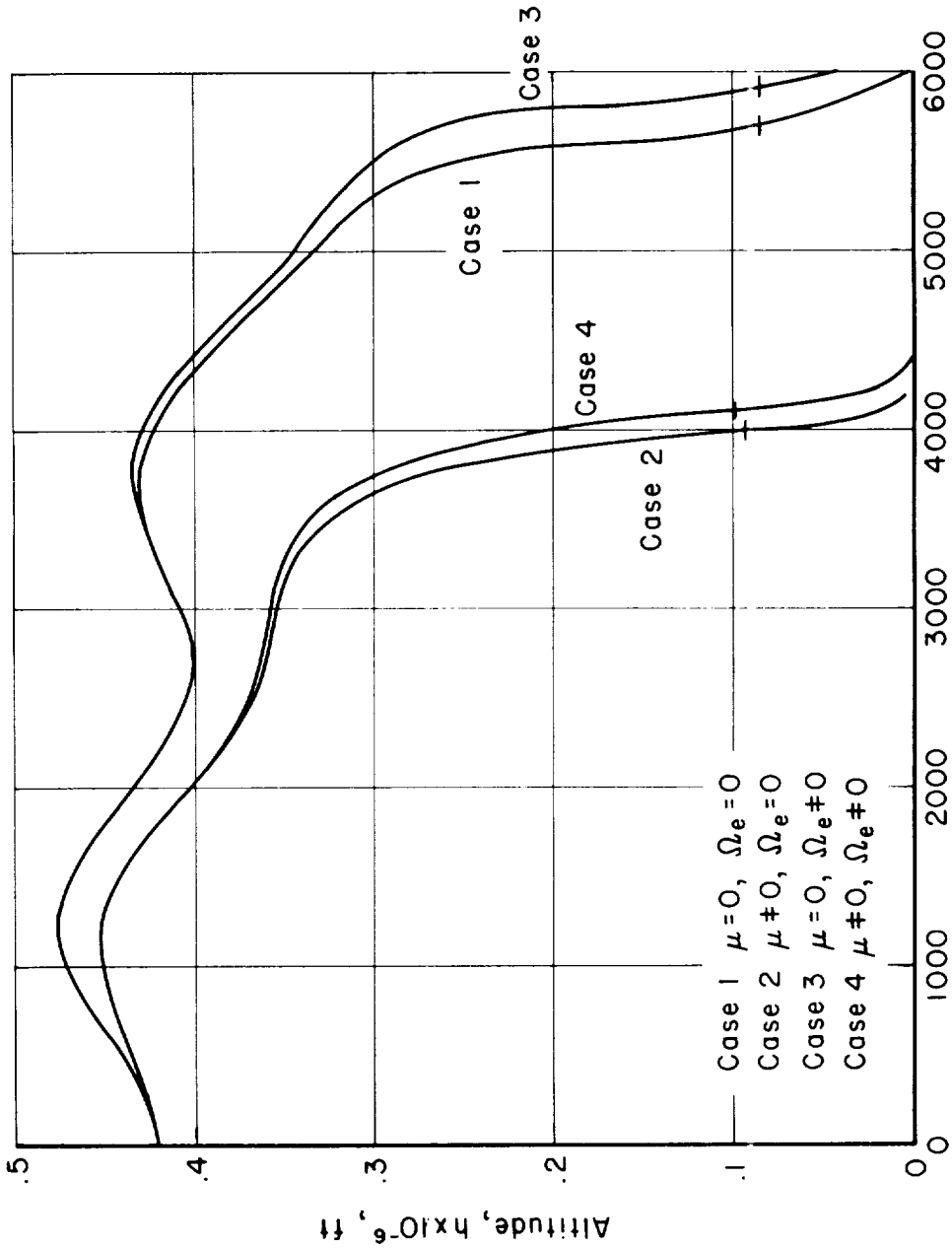

(a) Altitude.

Figure 7.- Trajectory of satellite launched from equator for all four cases; $C_DA/m = 1$; $\dot{r}_o = 0$, $\alpha_o = 65^\circ$.

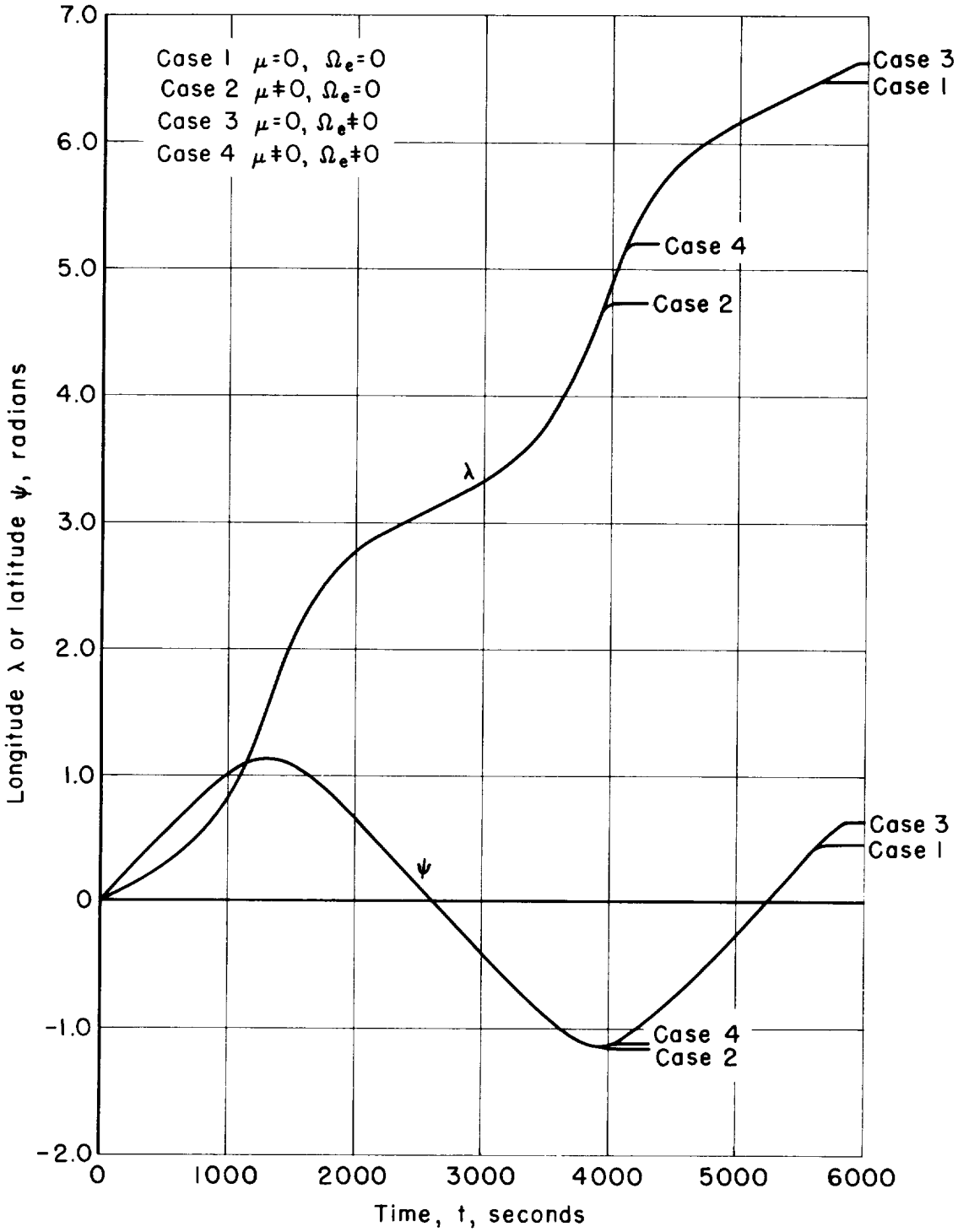

(b) Latitude and longitude.

Figure 7.- Continued.

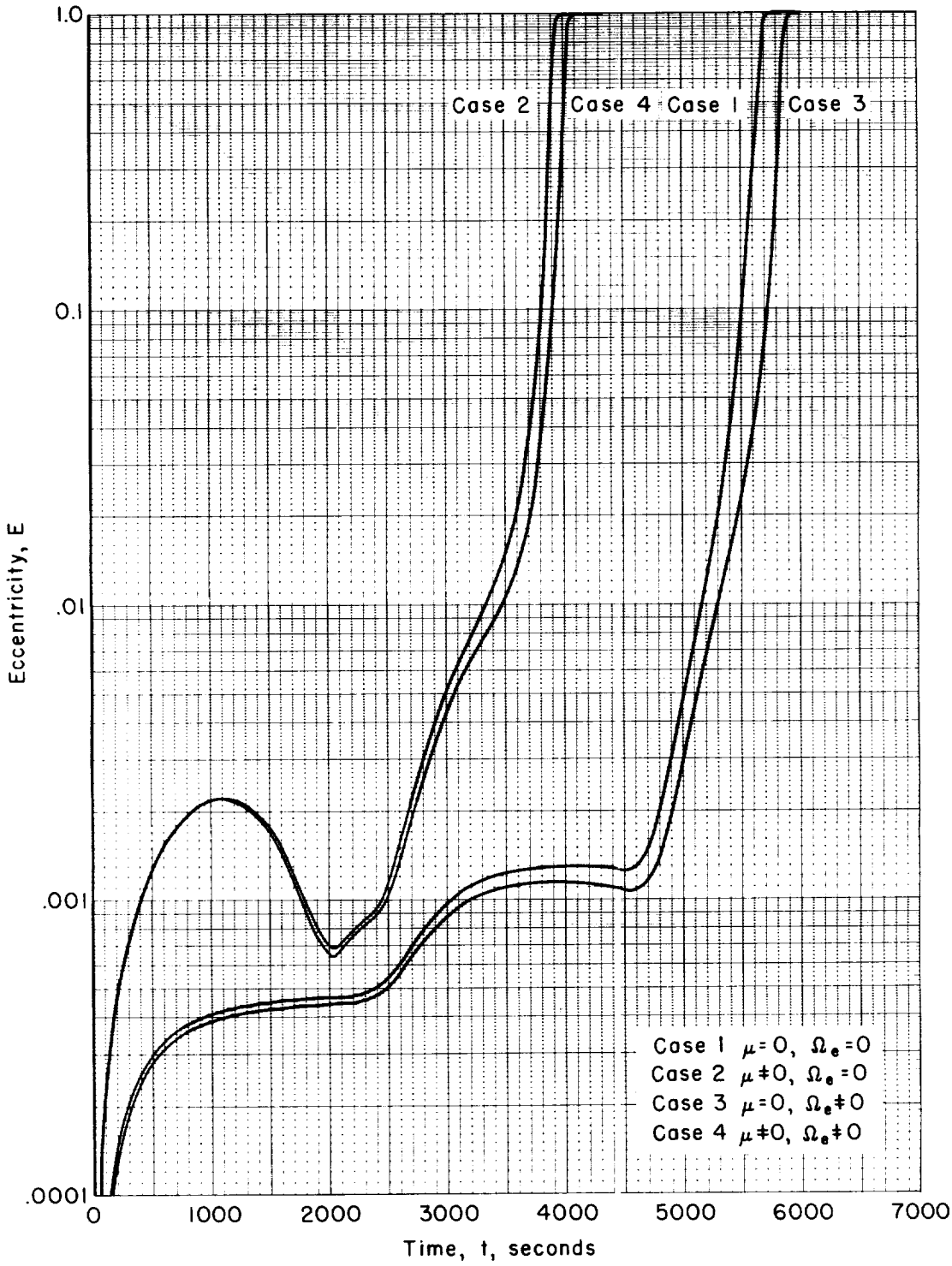

(c) Eccentricity.

Figure 7.- Concluded.

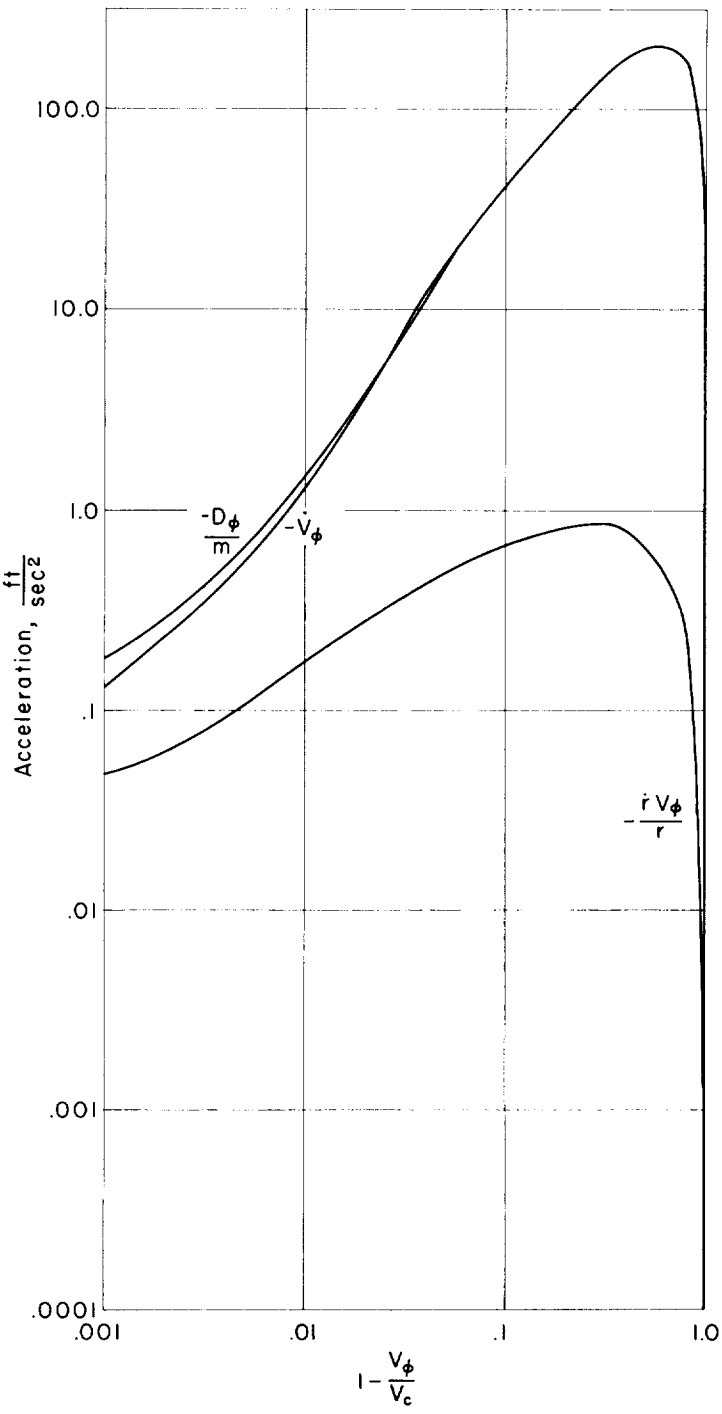

(a) $C_DA/m = 1$; $\dot{r}_o = 0$.

Figure 8.- Order of magnitude of various terms in equation of tangential motion; case 1, $\Omega_e = 0$, $\mu = 0$.

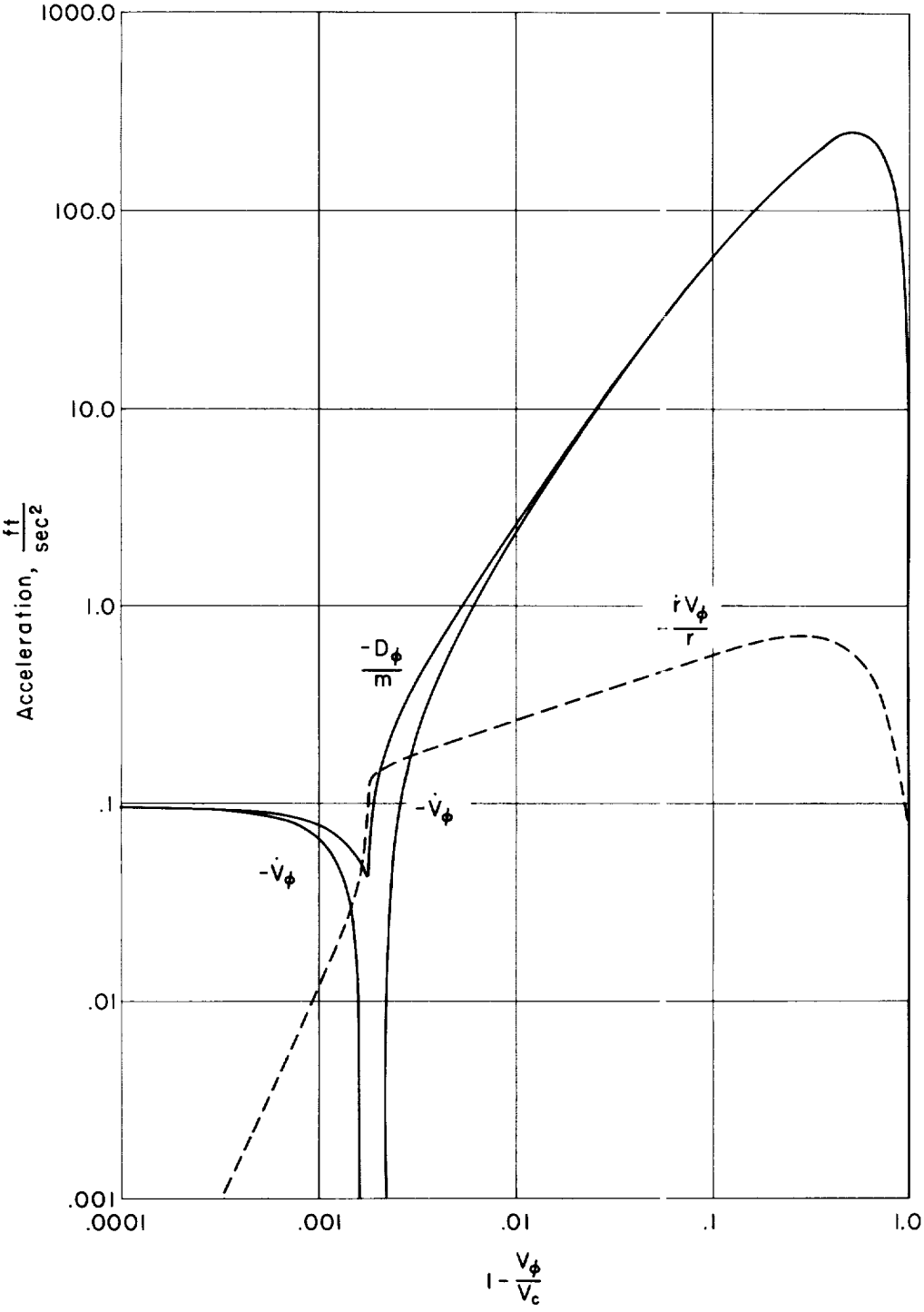

(b) $C_DA/m = 10$; $\dot{r}_o = 0$.

Figure 8.- Continued.

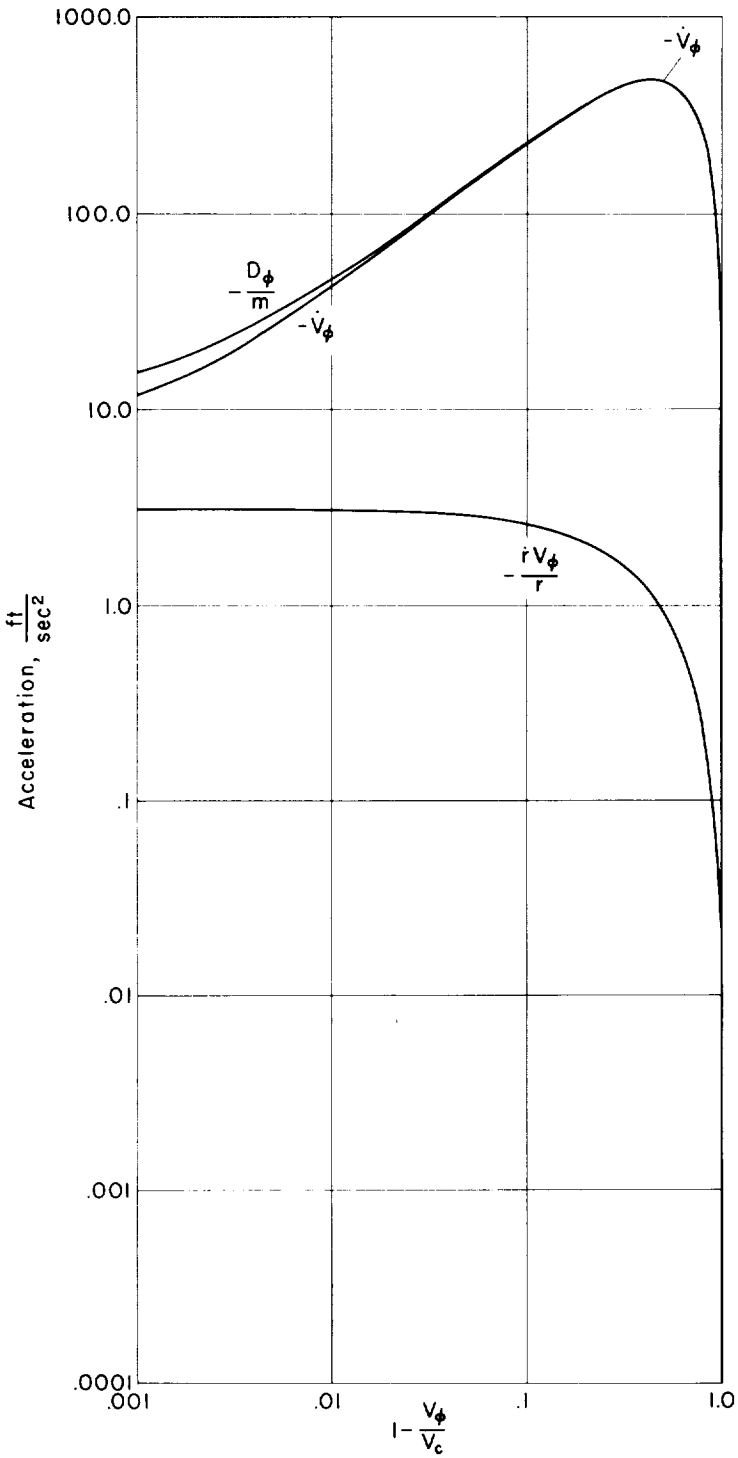

(c) $C_D A/m = 1$; $\dot{r}_o = -0.1(V_\varphi)_o$.

Figure 8.- Concluded.

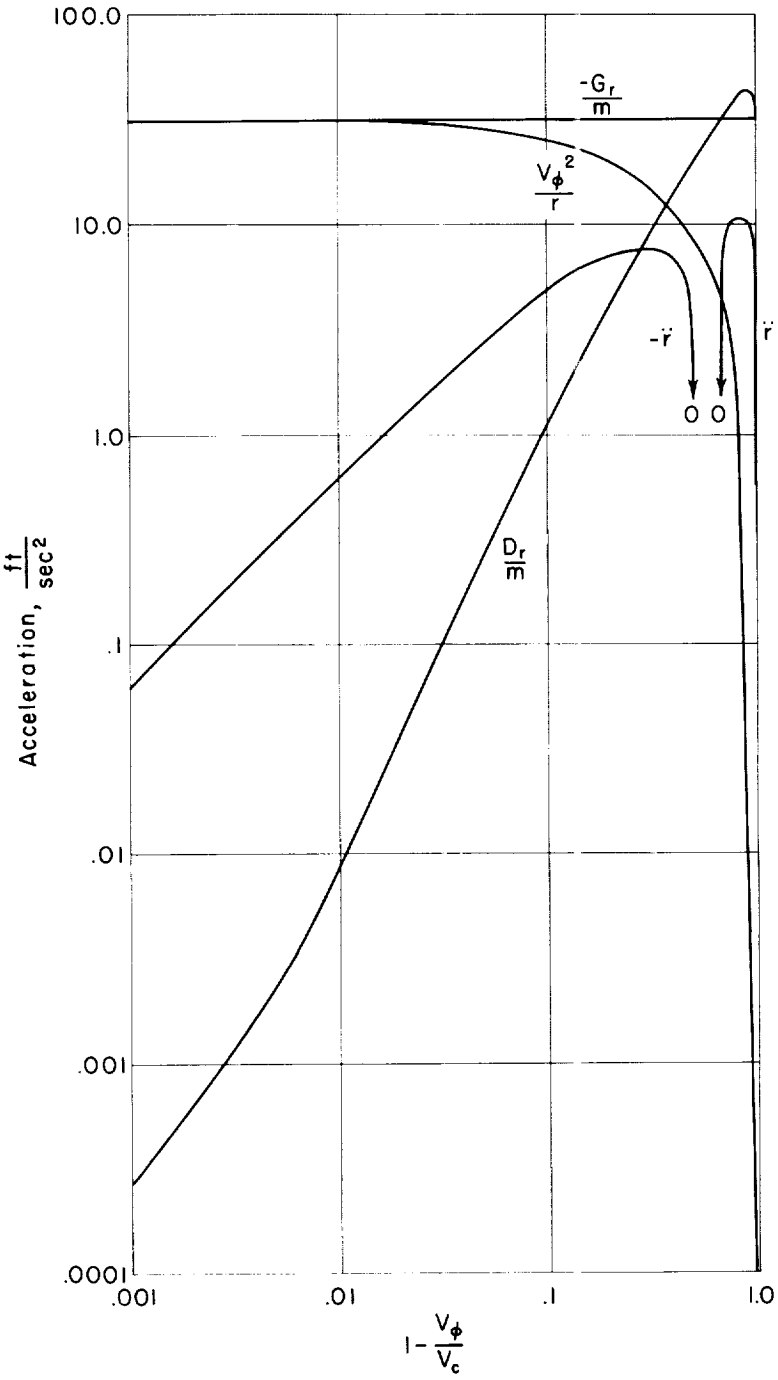

(a) $C_D A/m = 1$; $\dot{r}_o = 0$.

Figure 9.- Order of magnitude of various terms in equation of radial motion; case 1, $\Omega_e = 0$, $a = 0$.

12-4-58A

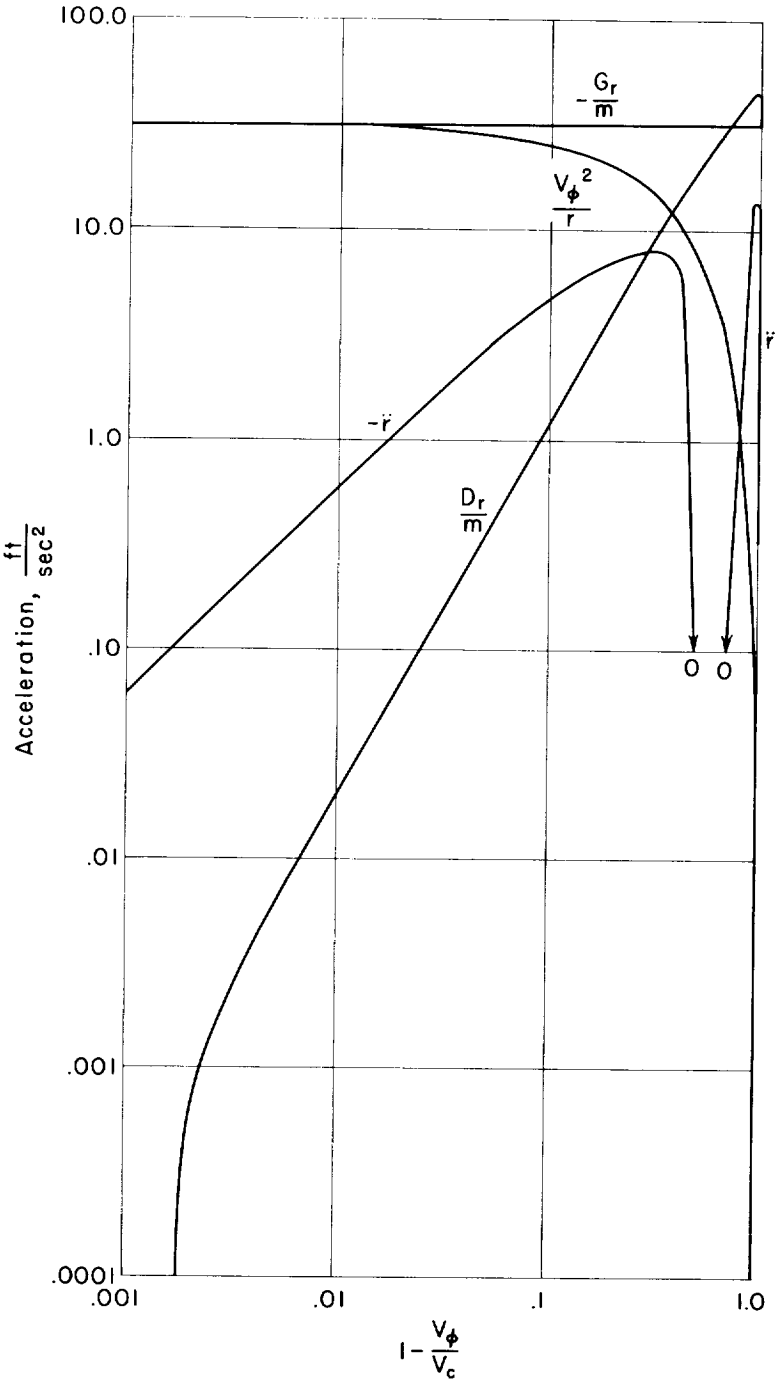

(b) $C_DA/m = 10$; $\dot{r}_o = 0$.

Figure 9.- Continued.

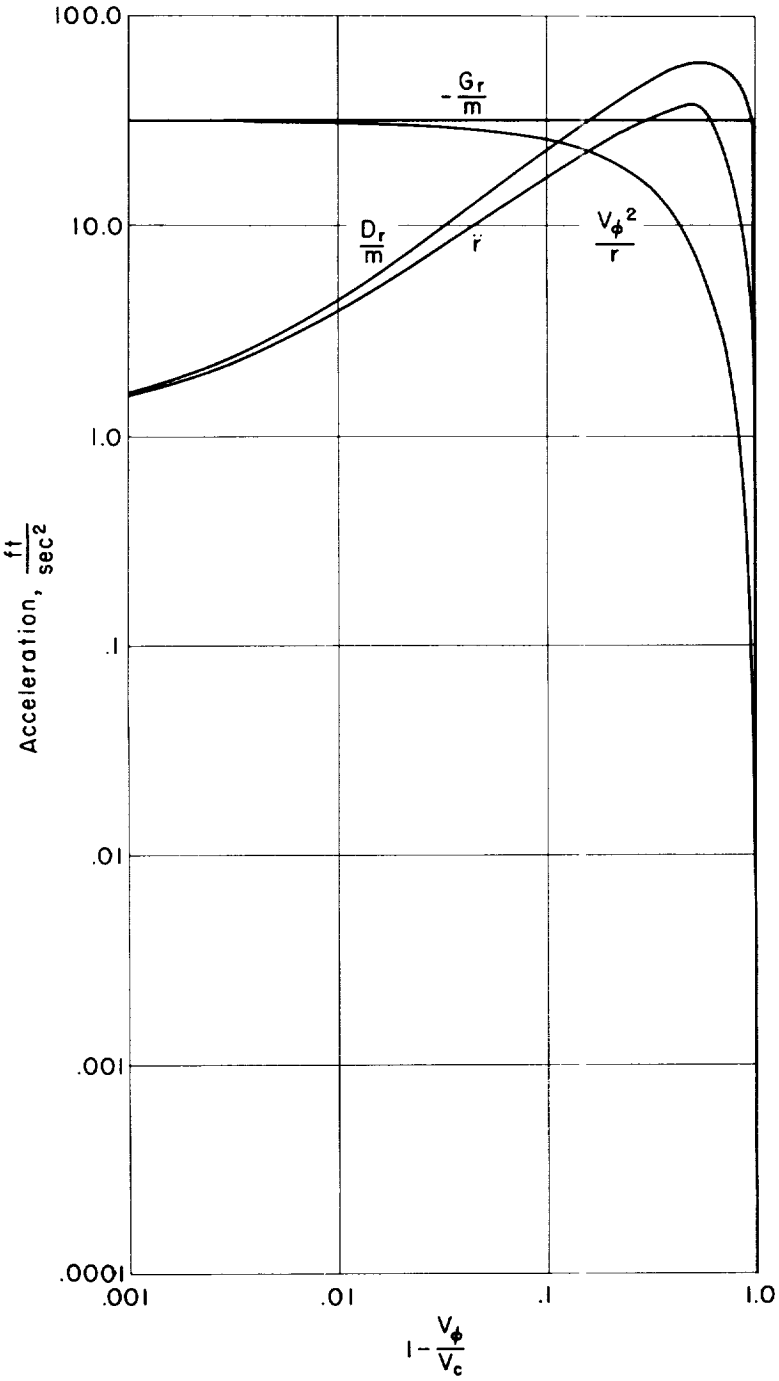

(c) $C_DA/m = 1$; $\dot{r}_o = -0.1(V_\varphi)_o$.

Figure 9.- Concluded.

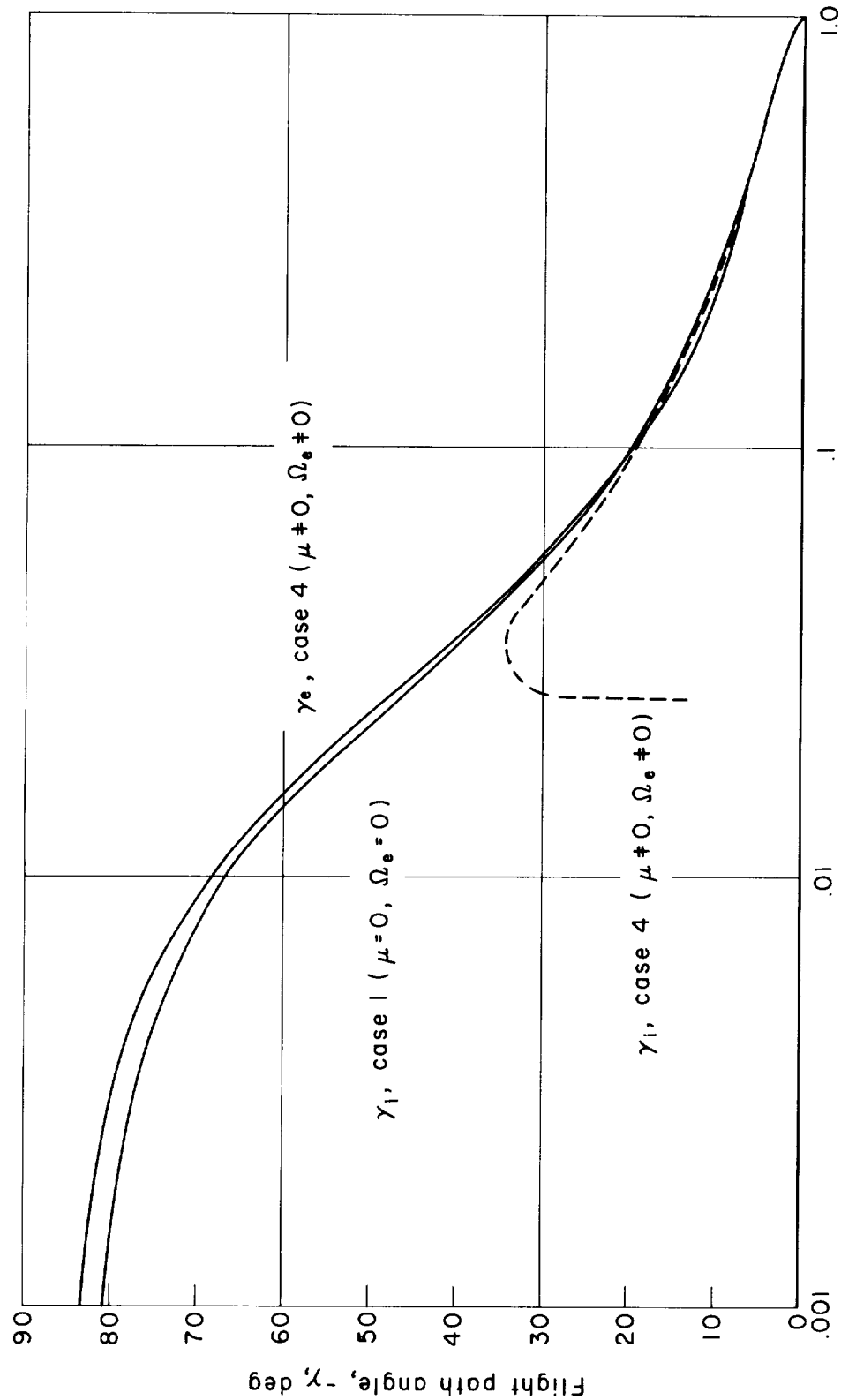

Figure 10.- Variation of flight path angle for various observers and conditions of flight; $\alpha_o = 65^\circ$, $C_DA/m = 1$, $h_o = 80$ statute miles.

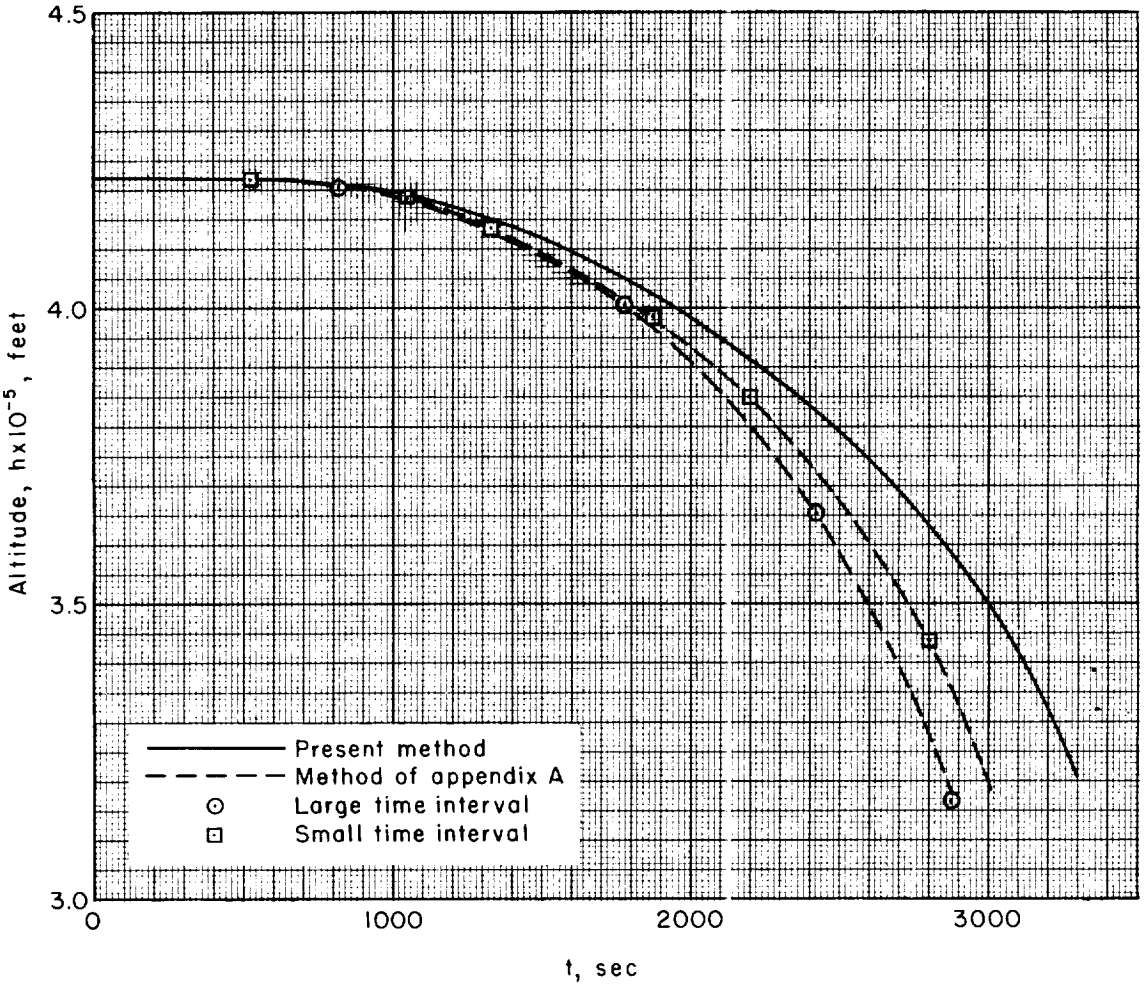

(a) Altitude.

Figure 11.- Comparison of approximate analytical trajectory and numerical trajectory during initial phase; $\alpha_o = 0^o$, $C_D A/m = 1$, $\Omega_e = 0$, $\mu = 0$, $h_o = 80$ statute miles.

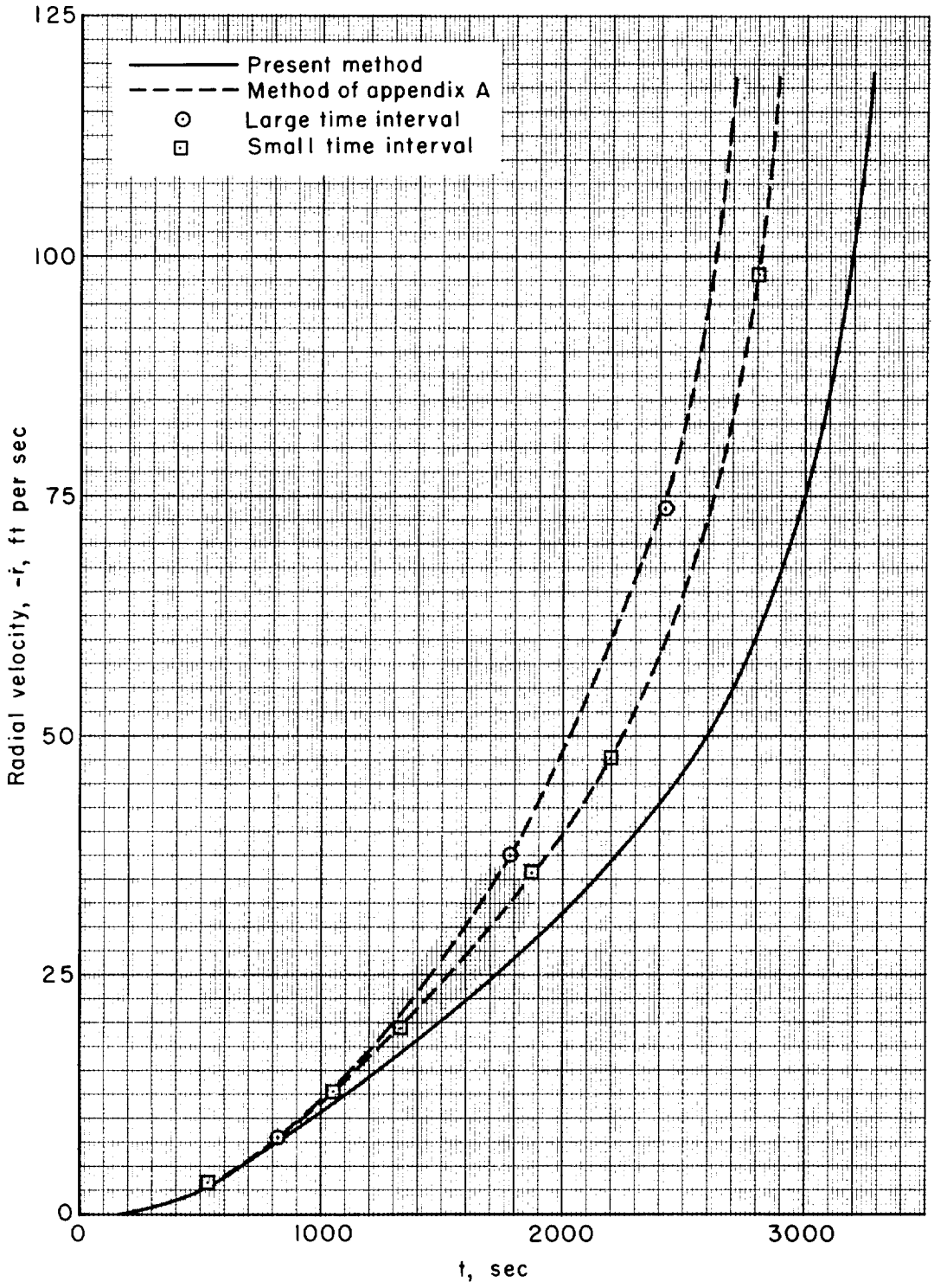

(b) Radial velocity.

Figure 11.- Concluded.

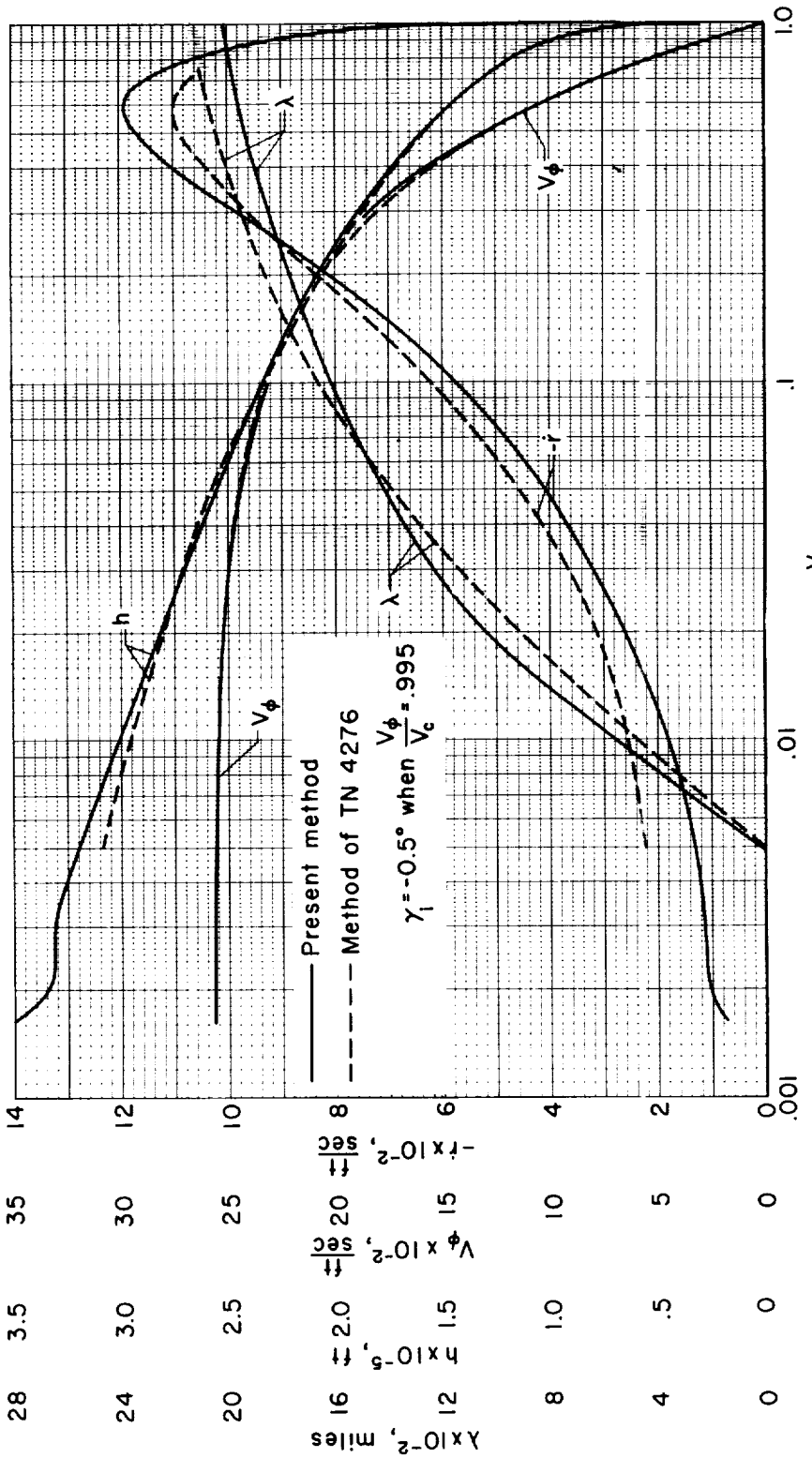

(a) Altitude, h; radial velocity, $\dot{r}$; horizontal velocity, V_φ; range, λ.

Figure 12.- Comparison of equatorial trajectory with mid-course trajectory calculated by method of NACA TN 4276 (ref. 4); $\alpha_o = 0^o$, $C_DA/m = 1$, $\Omega_e = 0$, $\mu = 0$, $h_o = 80$ statute miles.

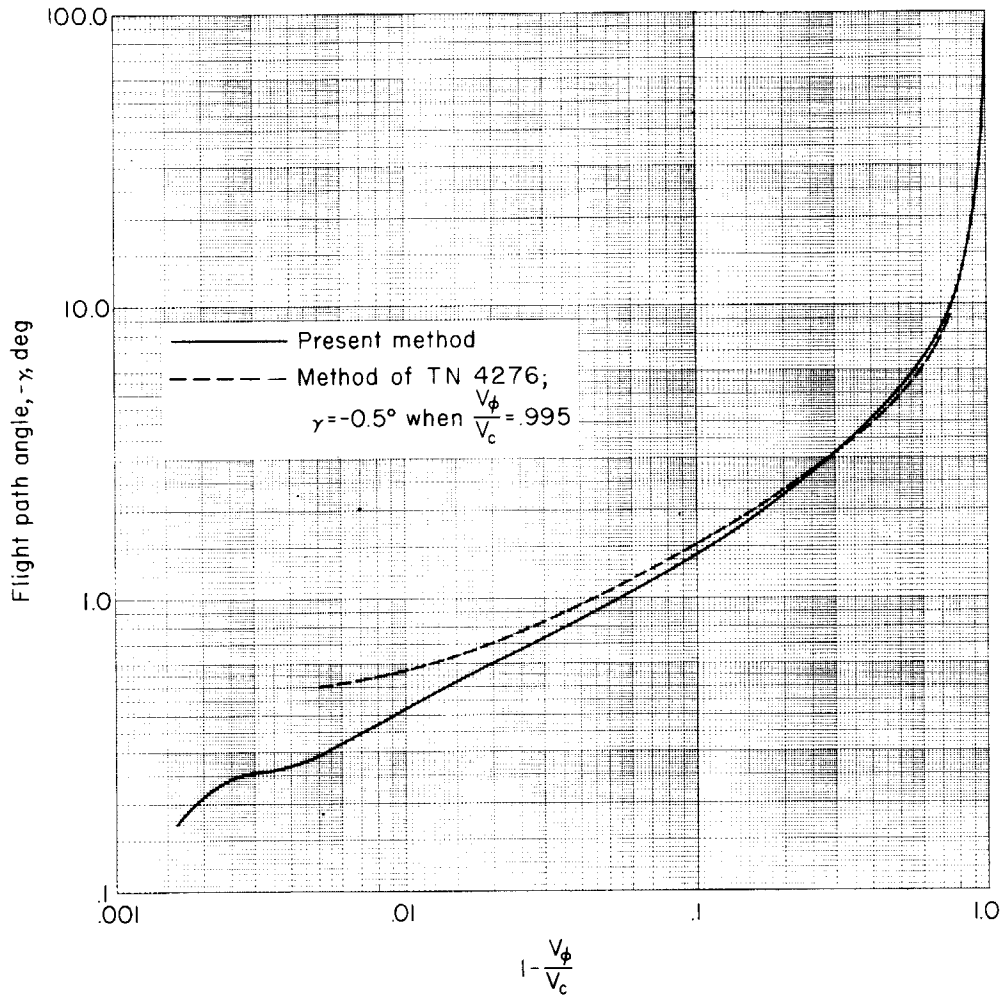

(b) Flight path angle, γ.

Figure 12.- Concluded.